NWRI CONTRIBUTION 85-138

Bishop (26)
Donelan (37)

This has been submitted to the forthcoming Handbook of Civil Engineering to be published by Technomic Publishing. The contents are subject to change.

WAVES AND WAVE FORECASTING

by

C.T. Bishop and M.A. Donelan

Shore Processes Section
Hydraulics Division
National Water Research Institute
Canada Centre for Inland Waters
P.O. Box 5050
Burlington, Ontario L7R 4A6

November 1985

TABLE OF CONTENTS

TABLE OF CONTENTS (cont'd)

ABSTRACT

Wind-generated waves and related topics are discussed in a handbook format suitable for a general civil engineer without an extensive background in hydraulics or coastal engineering. Linear wave theory is presented assuming monochromatic waves, and then is related to irregular waves. Basic wave processes, such as refraction, diffraction, reflection, shoaling and breaking, are reviewed. Techniques for the measurement of waves and wave direction are summarized. Wave statistics and methods of analysis are explained. Finally, simple methods of wave prediction are described for application with nomographs or hand-held calculators.

RÉSUMÉ

On étudie les vagues produites par le vent et des sujets connexes dans une brochure conçue à l'intention d'ingénieurs civils qui ne possèdent pas de grandes connaissances générales en hydraulique ou en génie côtier. On présente la théorie des vagues linéaires en fonction d'ondes monochromatiques, puis par rapport aux vagues irrégulières. Les procédés fondamentaux de la formation des vagues, par exemple la réfraction, la diffraction, la réflexion, le seuil et le déferlement, sont étudiés. On résume les techniques employées pour mesurer les vagues et leur direction. On explique les statistiques sur les vagues et les méthodes d'analyse. Enfin, on décrit des méthodes simples servant à prévoir les vagues pour les appliquer aux nomoprogrammes ou aux calculatrices portatives.

MANAGEMENT PERSPECTIVE

Measurement and analysis of wind generated surface waves has advanced significantly in the last decade. This report gives the text for an engineering handbook scheduled for publication. The text is written for use by engineers and includes material not included in current text books.

Anyone needing a quick reference before obtaining measurement or analysing surface wave records should become familiar with this contribution.

T. Milne Dick
Chief
Hydraulics Division

PERSPECTIVE-GESTION

On a fait beaucoup de progrès, au cours de la dernière décennie, dans le domaine de la mesure et de l'analyse des vagues de surface produites par le vent. Le présent rapport donne le contenu d'une brochure technique que l'on prévoit de publier. Le texte est écrit de façon à pouvoir être utilisé par des ingénieurs et renferme des renseignements que ne fournissent pas les ouvrages actuels.

Toute personne qui a besoin d'une référence rapide avant d'obtenir la mesure des vagues de surface ou d'analyser les relevés de ces dernières devrait prendre connaissance de cet ouvrage.

Le chef,

T. Milne Dick
Division de l'hydraulique

1.0 INTRODUCTION

This section is devoted to one type of surface water waves, usually known as gravity waves or wind generated waves. Waves can be defined as undulations of the water surface. The subject of water waves covers phenomena from capillary waves, which are very small and have very short periods (of the order of 0.05 seconds), to long period waves, such as tides, tsunamis and others which can reach magnitudes of the order of 10 m (in shallow water) and have long periods (of the order of minutes or hours). Gravity waves produced by the wind have typical periods of 0.3 to 30 seconds and wave heights mostly of the order of 1 metre, seldom exceeding 20 m. These wind waves account for a major part of the total surface wave energy and are usually the most important in coastal engineering and structural design.

1.1 Sea and Swell

The wind is the primary generating force for gravity waves. Other important factors include the fetch (open water distance over which the wind blows), the duration of the storm, and the depth of water. Wind waves can be separated into sea and swell. Waves are known as seas within the local wind generating area. When these waves travel out of the local wind generating area, so that they are no longer subject to significant wind input, they are known as swell. Seas contain waves of many different heights, periods and directions and can appear to be very complex. As waves travel out of the generating area the components of the sea disperse and attenuate at different rates. Short waves decay more quickly so that swell has a more uniform and long-crested nature than does sea. At some distance from the generating area the dispersion (long waves travelling faster than short waves) separates the components. Accordingly, a time history of swell approaching from a distant storm reveals a narrow spectrum (most waves

having nearly the same frequency) in which the mean frequency slowly increases because the slower short (higher frequency) waves arrive later. At the same time, the energy of all the waves is dissipated to some extent with the result that swell has a more orderly pattern than sea, with longer wave periods, smaller wave heights and a more uniform direction.

2.0 WAVE THEORY

This section presents the simplest of wave theories, assuming monochromatic waves. This theory forms the building blocks from which actual random waves and wave processes can be analyzed.

2.1 Definitions

Figure 1 shows the basic description of a simple sinusoidal progressive wave consisting of its wavelength L (the horizontal distance between corresponding points on two successive waves), height H (the vertical distance between a crest and the preceding trough), period T (the time for two successive crests to pass a given point), and water depth d (the distance from the bed to the stillwater level SWL). If the water surface η varies sinusoidally it can be defined as:

$$\eta = a \cos\theta \qquad (1)$$

where a = wave amplitude = H/2 for small-amplitude theory

$\theta = 2\pi\left(\frac{x}{L} - \frac{t}{T}\right)$ = phase angle

x = horizontal coordinate of the water surface

t = time.

A wave is periodic if its motion and surface profile recur in equal intervals of time. A waveform which moves relative to a fixed point is called a progressive wave; the direction in which it moves is termed the direction of wave propagation. Water waves are considered oscillatory if the water particle motion is described by orbits that are closed for each wave period. Small-amplitude wave theory (also known as linear theory, Airy theory, first order theory) developed by Airy in 1845 describes pure oscillatory, periodic, progressive waves. In most straightforward civil engineering designs, the small-amplitude theory is adequate.

Most finite-amplitude wave theories describe nearly-oscillatory waves because the fluid is moved a small amount in the direction of wave propagation by each successive wave. This motion yields mass transport by the waves. The main finite-amplitude theories are Stokes, Stream Function, Cnoidal and Solitary. For larger wave heights (finite-amplitude waves) in constant depth the Stokes theory (Stokes 1847) or Stream Function theory (Dean 1974) can be used. In shallower and shoaling water Cnoidal wave theory can be used (Korteweg and deVries 1895). In very shallow water, as waves are about to break, Solitary wave theory (McCowan 1891) can be used. The ranges of applicability of each theory are summarized in Figure 2. The expressions given in this section are applicable to small amplitude waves (no mass transport).

2.2 Wave Celerity

The velocity of the waveform in relation to the body of fluid through which the wave propagates is termed the wave celerity C. The celerity is such that the phase function θ of Equation 1 remains constant and thus is related to wavelength and period by:

$$C = \frac{L}{T} \tag{2}$$

The small-amplitude wave theory expression for celerity versus wavelength is:

$$C = \left\{ \frac{gL}{2\pi} \tanh \frac{2\pi d}{L} \right\}^{1/2} \tag{3}$$

In deep water, $d/L \geq 0.5$, the value of $\tanh 2\pi d/L$ approaches 1.0 (Figure 3) and the previous equation reduces to

$$C_0 = \left\{ \frac{gL_0}{2\pi} \right\}^{1/2} = \frac{L_0}{T} \tag{4}$$

where the subscript "0" indicates deep water conditions. The period T remains essentially constant and independent of depth for oscillatory waves. In deep water, all the wave characteristics are virtually independent of depth. In shallow water, $d/L \leq 0.04$, Equation 3 reduces to:

$$C = \sqrt{gd} \tag{5}$$

The water depth is considered to be transitional when $0.04 < d/L < 0.5$.

2.3 Wavelength

From Equations 2 and 3, an expression for wavelength may be obtained.

$$L = \frac{gT^2}{2\pi} \tanh \frac{2\pi d}{L} = L_0 \tanh \frac{2\pi d}{L} \tag{6}$$

Equation 6 can be solved using Figure 4 or can be rearranged to give:

$$\frac{d}{L_0} = \frac{d}{L} \tanh \frac{2\pi d}{L} \tag{7}$$

This equation can be solved most easily using published tables (Shore Protection Manual 1984; Wiegel 1964) of d/L and d/L_0, or with the help of Figures 3 and 5.

An approximate expression for Equation 6 given by Eckart (1952) (also Shore Protection Manual 1984) is:

$$L \approx \frac{gT^2}{2\pi} \left(\tanh\left(\frac{4\pi^2}{T^2} \frac{d}{g}\right)\right)^{1/2} \tag{8}$$

The maximum error from using Equation 8 is 5 percent, occurring when $2\pi d/L \approx 1$.

In deep water, Equation 6 reduces to:

$$L_0 = \frac{gT^2}{2\pi} \tag{9}$$

2.4 Orbital Motion

The water particles in a wave move in orbital paths as shown in Figure 6. The horizontal component u and the vertical component w of the local fluid velocity are given by:

$$u = \frac{\pi H}{T} \frac{\cosh k(z+d)}{\sinh kd} \cos\theta \tag{10}$$

and

$$w = \frac{\pi H}{T} \frac{\sinh k(z+d)}{\sinh kd} \sin\theta \tag{11}$$

where $k = 2\pi/L$ = wavenumber

and z = vertical distance measured positive upward from the mean water level.

The corresponding expressions for orbital acceleration are:

$$\frac{\partial u}{\partial t} = \frac{2\pi^2 H}{T^2} \frac{\cosh k(z+d)}{\sinh kd} \sin\theta \tag{12}$$

and

$$\frac{\partial w}{\partial t} = -\frac{2\pi^2 H}{T^2} \frac{\sinh k(z+d)}{\sinh kd} \cos\theta \tag{13}$$

Water particle displacements can be characterized by A and B

where

$$A = \frac{H}{2} \frac{\cosh k(z+d)}{\sinh kd} \tag{14}$$

and

$$B = \frac{H}{2} \frac{\sinh k(z+d)}{\sinh kd} \tag{15}$$

A is the major (horizontal) semiaxis of an ellipse with the minor (vertical) semiaxis equal to B. The lengths A and B are measures of the horizontal and vertical displacements of the water particles.

In deep water:

$$A_0 = B_0 = \frac{H}{2} e^{kz} \tag{16}$$

and the orbits are circular.

In shallow and transitional water the orbits are elliptical. The shallower the water, the flatter the ellipse becomes. At the bottom the water motion is entirely horizontal.

2.5 Subsurface Pressure

Subsurface pressure beneath a wave consists of a static component, ρgz, due to the hydrostatic pressure, and a dynamic component due to fluid acceleration, giving

$$p = \rho g \frac{H}{2} \frac{\cosh k(d+z)}{\cosh kd} \cos\theta - \rho gz \qquad (17)$$

where p = gauge pressure = total pressure - atmospheric pressure. The expression

$$\frac{\cosh k(d+z)}{\cosh kd} \qquad (18)$$

is normally known as the pressure response factor, K_p. The dynamic pressure fluctuations are attenuated with depth as a function of wave period. The water column tends to filter out the higher frequency components of the pressure fluctuations. Equation 17 can be rearranged to give:

$$\eta = \frac{1}{K_p} \left(\frac{p}{\rho g} + z\right) \qquad (19)$$

2.6 Group Velocity

The speed of a group of waves, travelling with a group velocity C_g, is generally not the same as the speed of individual waves, travelling at a wave celerity or phase velocity C. The concept of group velocity can be described by considering the interaction of two sinusoidal wave trains moving in the same direction with slightly different wavelengths and periods. Assume, for simplicity, that the heights of both components are equal. Since the wavelengths of the two component

waves are assumed to be slightly different, for some values of x at a given time, the two components will be in phase and the observed wave height will be 2H. For some other values of x, the two waves will be completely out of phase and the resultant wave height will be zero. The waves shown in Figure 7 appear to be travelling in groups.

It is the velocity of these groups that represents the group velocity, given by

$$C_g = nC \tag{20}$$

where $$n = \frac{1}{2}\left[1 + \frac{4\pi d/L}{\sinh (4\pi d/L)}\right] \tag{21}$$

Values of n can be found in tables or from Figure 8. In deep water the group velocity is one-half the wave celerity. In shallow water, the group velocity equals the wave celerity. Wave energy is propagated at the group velocity.

2.7 Wave Energy

The total energy of a wave system is the sum of its kinetic energy and its potential energy. According to small amplitude wave theory, if the potential energy is calculated relative to the still water level and all waves are propagating in the same direction, potential and kinetic energy components are equal. Then the total wave energy in one wavelength per unit crest width is

$$E_T = E_k + E_p = \frac{\rho g H^2 L}{16} + \frac{\rho g H^2 L}{16} = \frac{\rho g H^2 L}{8} \tag{22}$$

Total average wave energy per unit surface area, termed the specific energy or energy density is

$$E = \frac{\rho g H^2}{8} \tag{23}$$

Wave energy flux per unit crest width is the rate at which energy is transmitted in the direction of wave propagation and is a vectorial quantity (denoted by a tilde) given by

$$\underset{\sim}{P} = E \underset{\sim}{C}_g \tag{24}$$

2.8 Random Waves

Wind waves are not monochromatic sinusoidal waves. However, the concept of a random sea made up of an infinite collection of infinitesimal sinusoids in random phase leads to a convenient spectral description that is amenable to engineering applicaitons. Since the pioneering work of Pierson and Marks (1952), spectral analysis of wave records has found more and more frequent application in oceanography and engineering.

Consider five wave trains of different heights and frequencies (inverse periods) summed together in random phase (Figure 9). A section of the resulting wave train is shown at the bottom of the figure. The (discrete) spectrum of variance with frequency for these five wave trains is represented by Figure 10. Natural waves are represented by a continuous spectrum, i.e., an infinite set of components each having infinitesimal energy (Figure 11).

Analysis of random seas yields a wave variance spectrum (Section 7.1) in which the wave variance spectral density $\Phi(f)$ is expressed as a function of frequency f. Wave energy density is related to the variance spectrum as:

$$E = \rho g \int_0^\infty \Phi(f)\, df = \rho g \sigma^2 = \frac{\rho g}{16} H_{m_0}^2 \qquad (25)$$

where the area under the variance spectrum is σ^2 and a characteristic wave height is defined as:

$$H_{m_0} = 4\sigma \qquad (26)$$

It is interesting to note that the energy density in a random sea with $H_{m_0} = H$ is only one-half of the energy density of a monochromatic wave train with wave height H.

3.0 WAVE PROCESSES

3.1 Wave Refraction and Shoaling

Equation 3 shows that for $d/L < 0.5$ the wave celerity depends on the water depth. As the wave celerity decreases with depth, so does the wavelength. When waves approach the shore in such a manner that the angle between the wave crests and the bottom contours is non-zero, the depth will vary along each wave crest. The parts of the wave in shallower water will move forward more slowly than those parts in deeper water. This variation causes the wave crest to bend toward alignment with the contours. This process is known as refraction. In addition to refraction caused by variations in bathymetry, waves may be refracted by currents or any other phenomenon causing one part of a wave to travel slower or faster than another part. Refraction is an important factor in determining local wave height and direction (see, for example, Pierson 1972).

The primary assumption in refraction analysis is that wave energy flux between orthogonals remains constant; orthogonals are lines drawn perpendicular to the wave crests and extend in the direction of

wave advance. In deep water the rate at which wave energy is transmitted forward across a plane between two adjacent orthogonals is

$$B_0 = \frac{1}{2} b_0 E_0 C_0 \tag{27}$$

where b_0 is the distance between the selected orthogonals in deep water. Since the energy flux between orthogonals is taken to be constant, this energy flux may be equated to the rate at which the energy is transmitted forward between the same two orthogonals in shallow water

$$B = n\, b\, E\, C = B_0 \tag{28}$$

where b is the spacing between the orthogonals in the shallower water. From Equations 23, 27, and 28, one obtains

$$\frac{H}{H_0} = \left(\frac{E}{E_0}\right)^{1/2} = \left(\frac{C_0}{2nC}\right)^{1/2} \left(\frac{b_0}{b}\right)^{1/2} \tag{29}$$

The term $\sqrt{C_0/2nC}$ is known as the shoaling coefficient K_s. It can be found in tables of d/L_0 or d/L (Shore Protection Manual 1984) or from Figure 12. It may be seen that, neglecting refraction, the wave height tends to decrease in shoaling water until near the breaking point, when it increases again.

The term $\sqrt{b_0/b}$ is known as the refraction coefficient K_r. Several graphical procedures for refraction analysis are available (Shore Protection Manual 1984).

The change of direction of an orthogonal as it passes over relatively simple bathymetry that can be approximated by parallel contours may be computed from Snell's law:

$$\sin \alpha_2 = \frac{C_2}{C_1} \sin \alpha_1 \qquad (30)$$

where α_1 = the angle a wave crest makes with the bottom contour over which the wave is passing.

α_2 = a similar angle measured as the wave crest passes over the next selected bottom contour.

C_1 = the wave celerity at the depth of the first contour.

C_2 = the wave celerity at the depth of the second contour.

For straight shorelines with parallel offshore contours, refraction and shoaling may be computed analytically or with the help of Figure 13. For more complex topography many computer methods are available to perform refraction analyses. These numerical methods can be very useful in determining wave refraction diagrams over a large area or when several different wave periods are of interest. Details for regular waves can be found in many references such as Wilson (1966) and Dobson (1967). In addition the Shore Protection Manual (1984) gives a detailed manual graphical procedure. A typical refraction diagram for monochromatic waves from one direction is shown in Figure 14.

The above discussion is applicable to monochromatic waves. Such conditions are approximately met by swell generated at great distance from an oceanic coast. In general, random (broad-band) wind seas must be treated differently. Two approaches are available: (1) detailed calculations of wave propagation (Karlson 1969) including generation of and interaction with shore-normal and longshore currents (Birkemeier and Dalrymple 1975, Tayfun et al. 1976); (2) separating the spectrum into several components, refracting each separately and recombining to yield the transformed spectrum (Goda 1985). The first method involves the use of time-stepping finite difference numerical models. The second method involves a linear decompositon of the spectrum into several discrete frequency bands. The choice of how many frequency

bands depends on the desired accuracy of the calculation - normally seven to ten are adequate if the bands are chosen to have equal energy (spectral variance) rather than equal spectral width. A single frequency (the centroid of this band with respect to spectral density) is associated with each band and the procedure for regular waves (outlined above) is applied to each band independently of the other spectral bands. The construction of wave rays from offshore towards the shore often leads to the occurrence of "caustics" (areas where adjacent rays cross); this can cause difficulties in interpreting the local wave height (Chao and Pierson 1972). Furthermore, a large number of rays must be constructed for various offshore approach directions in order to yield wave heights at particular inshore locations. Also, the inshore conditions are highly sensitive to topographic features and to small changes in offshore conditions. In order to reduce the number of ray trajectory calculations, Dorrestein (1960) suggested constructing rays from the inshore location of interest towards the offshore. This method has been developed into a general refraction computer method for directional wave spectra by Abernethy and Gilbert (1976). The use of spectra with some directional spread, rather than long crested waves, reduces the problem of caustics and smoothes the results making them less sensitive to small topographic irregularities and to changes in offshore approach directions.

Since changes in water depth affect the refraction calculations, the results of refraction analyses depend on phase and amplitude of the tide and on storm surges, seiches and longer term water level changes such as seasonal lake level fluctuations. In general, refraction calculations should be performed for the maximum and minimum expected (over the life of the proposed structure) water levels as well as the mean. Furthermore, when refraction calcualtions are carried out over large distances (>50 km) the curvature of the earth must be considered (Chao 1972).

For further information on numerical refraction of wave spectra refer to Abernethy and Gilbert (1975), Brampton (1981) and Goda (1985).

3.2 Diffraction

Diffraction of water waves is the phenomenon by which energy is radiated from the point of interception of a wave train by a barrier, such as a breakwater. The effect of diffraction is shown by waves propagating into the sheltered region within the barrier's geometric shadow. Diffraction is important in determining wave height distribution within harbours or sheltered bays, or in the lee of islands.

Wave diffraction diagrams have been calculated on the basis of Sommerfeld's (1896) diffraction theory as extended or applied by Penny and Price (1944), Blue and Johnson (1949) and Wiegel (1962). Wave height reduction is given in terms of a diffraction coefficient K_d defined as the ratio of local diffracted wave height H to the incident wave height H_i unaffected by diffraction. Diagrams are available for different angles of approach at 15 degree intervals (Shore Protection Manual 1984). Figure 15 shows the diffraction diagram for waves approaching normal to the breakwater. Overlay templates of these diagrams can be scaled to correspond to the hydrographic chart being used.

Diffraction diagrams are also available for waves passing a gap of width less than five wavelengths at normal incidence (Johnson 1952, Shore Protection Manual 1984). The diagram for a gap of width B = 2L is shown in Figure 16. If the gap width is greater than 5L, diagrams for a single breakwater may be used. An approximate determination of diffracted wave characteristics for oblique incidence may be obtained by considering the gap to be as wide as its projection in the direction of incident wave travel.

Diffraction around an offshore island or structure has been dealt with by Harms (1979).

The use of these diffraction diagrams calculated for monochromatic waves should be restricted to very narrow band swell. As for refraction and shoaling, when broad-band wind seas are being considered, it is necessary to treat the spectrum as a whole rather than a "significant (regular) wave" representation of it. As before, the spectrum is partitioned into equal variance bands, each of which is diffracted separately and finally recombined. The resulting diffraction diagrams for moderately narrow band (swell) and broad band (wind sea) spectra normally incident to a semi-infinite breakwater and a breakwater gap are shown in Figures 17 and 18 respectively. The differences are apparent between these diffraction diagrams for random seas and the corresponding diagrams (Figures 15 and 16) for a monochromatic train of waves.

3.3 Reflection

Water waves may be either partially or totally reflected from walls and other barriers. For incident angles (the angle between the direction of wave advance and the wall) greater than 45 degrees, waves reflect from a vertical wall in such a manner that the angle of incidence is equal to the angle of reflection. Depending on the wall's rigidity and porosity, reflections can take place with very little loss in energy. Consequently, in a harbour with insufficient wave energy absorbers, multiple wave reflections can result in a buildup of wave energy, manifested as wave agitation.

A barrier's reflection coefficient is given by the ratio of the reflected wave height H_r to the incident wave height H_i. Smooth impermeable vertical walls typically have reflection coefficients close to 1.0. Waves approaching in a direction perpendicular to such a wall can form a standing wave or clapotis, having a maximum height of $2H_i$ where the water surface is shown in Figure 19 and is given by:

$$\eta = H_i \cos \frac{2\pi x}{L} \cos \frac{2\pi t}{T} \tag{31}$$

For certain values of x, the water surface remains at the SWL (i.e., $\partial\eta/\partial t = 0$ for all t). These points are called nodes and are located a distance x_{node} from the vertical barrier, where:

$$x_{node} = (\frac{2n + 1}{4})L \quad , \quad n = 0,1,2,... \tag{32}$$

and L is the wavelength of the incident wave. At the nodes water motion is always horizontal. On erodible beds these areas are prone to erosion.

At antinodes, located a distance L/4 from nodes, the water surface excursion is $2H_i$ and the water motion is always vertical.

The reflection coefficient for waves approaching at right angles to plane slopes, beaches, and rubblemound revetments and breakwaters can be estimated from Figure 20 as a function of the surf similarity parameter

$$\xi = m \sqrt{L_0/H_i} \tag{33}$$

where m is the slope the beach or structure makes with the horizontal. The curves show that the wave reflection coefficient decreases as either the wave steepness increases or as the slope decreases.

For incident angles between 20 and 45 degrees, so-called Mach stem reflection (Wiegel 1964) occurs in which the interaction of the wave with the wall is a combination of reflection and diffraction. The resulting reflected wave travels parallel to the wall, increasing in height as it travels, and sometimes reaching a height several times that of the incident wave (Berger and Kohlhase 1976).

For incident angles less than 20 degrees, the wave crest bends so that it becomes perpendicular to the wall and no reflected wave appears.

3.4 Breaking

The maximum height of a wave in deep water occurs when the water particle velocity at the wave crest just equals the wave celerity. This corresponds to a limiting wave steepness (Michell 1893) of

$$\frac{H_0}{L_0} = 0.142 \approx \frac{1}{7} \tag{34}$$

and occurs when the crest angle is 120 degrees.

As a wave propagates into shoaling water depths, the limiting steepness which it can attain decreases, and has been found to depend on the relative depth d/L and the beach slope m perpendicular to the direction of wave advance. The breaking wave height H_b is related to the unrefracted deep water wave height H'_0 as shown in Figure 21. The depth of water at breaking d_b is related to H_b as shown in Figure 22 (this is sometimes simplified to $H_b/d = 0.78$ from Solitary Wave theory).

The preceding results are for monochromatic waves. For random waves, field measurements (Tucker et al. 1983, Thornton and Guza 1982, Thompson 1980) and laboratory measurements (Vincent 1985) have shown that the limiting value of H_{m_0}/d varies from 0.55 to 0.65. For most engineering purposes, a value of 0.6 can be used (Hughes 1984). An approach to determining the statistical distribution of heights in shallow water is given in Section 6.3.

3.5 Limiting Wave Energy Levels in Shoaling Water Depths

Bouws et al. (1985) have produced a universal equilibrium spectral form for wind seas called the TMA spectrum valid for all water depths. A simple expression for H_{m_0} has been derived from the TMA spectral form (Hughes 1984, Vincent 1982) which allows the prediction of the depth-limited equilibrium H_{m_0} in either intermediate or shallow water.

$$H_{m_0} = \frac{L\alpha_1}{\pi}^{1/2} \tag{35}$$

where L = wavelength associated with f_p (from linear theory)

$$\alpha_1 = 0.019 \left(\frac{U_{10}^2}{gL}\right)^{0.49} \tag{36}$$

and U_{10} = windspeed at 10 m elevation.

The main assumption invoked when using the TMA spectrum is that the wind sea is at a steady state or equilibrium condition. Therefore, Equation 35 is not valid for fetch- or duration-limited wave conditions (if used it would provide a conservative estimate). Furthermore, use of Equation 35 assumes that the bottom topography is a gentle slope (1:100 or flatter) with smoothly varying features such that refraction and diffraction effects are negligible.

3.6 Design Approach for Irregular Waves

Goda (1976, 1985) has provided a coherent procedure for dealing with random seas approaching offshore structures or coastlines.

Here we briefly summarize Goda's procedure with reference to his schematic diagram (Figure 23). The procedure starts from the generation of wind waves in deep water and follows them through dispersion, diffraction, refraction, shoaling and breaking to their final interaction with structures and coastlines. In this chapter the various natural wave modification processes outlined in Figure 23 are described. However the panels at the bottom of the figure, dealing with the interaction of waves with engineering structures, are discussed in a separate chapter. Five analysis methods are considered: (A) significant wave representation, (B) highest wave representation, (C) probability calculation, (D) irregular wave experiments, (E) spectral calculations. The types of analysis appropriate to a particular stage of the procedure are indicated by the letters A to E on the figure. Some types of analysis are quite general but require considerable calculation, while others are quite simple and generally highly idealized so that their range of suitability is quite restricted.

(A) The significiant wave representation amounts to assuming the existence of a train of regular (long crested) waves having (fixed) height and period equal to the significant height and period of the random sea. The virtue of this method lies in its simplicity. The drawback is that it can lead to large errors in certain situations, e.g., the diffraction of irregular waves or in the design of structures that may be sensitive to waves larger than the significant wave.

(B) The highest wave representation is akin to the significant wave representation except that the height and period of the highest wave replace those of the significant wave in the hypothetical regular wave train. This method leads to conservative design and is commonly used in the design of offshore structures where personnel safety is paramount. These are the idealized methods of dealing with irregular waves. The other methods (C to E) recognize the essential random character of natural waves.

(C) The probability calculation method relies on observed or theoretical joint distributions of heights and periods of individual waves. This method is particularly useful in cases where the cumulative effect of small changes is of interest rather than catastrophic failure due to a single large wave. Such problems as wave overtopping of a seawall and the working of breakwater components are suitably handled by the probability calculation method. Pierson and Holmes (1965) have devised a method of this type for dealing directly with the probability distribution of forces on structures.

(D) The irregular wave test method employs physical modelling techniques to simulate (on a smaller scale) the expected irregular wave conditions at the design site. The method requires sophisticated laboratory equipment. The best design method would be to test the model with a representative series of design spectra, suitably scaled by Froude's law. Many non-linearities are then properly scaled.

(E) The spectral calculation method recognizes that surface elevation changes are distributed among various frequencies (periods or wavelengths) and that decomposition into spectral components facilitates many frequency (or wavelength) dependent calculations such as refraction, diffraction, shoaling, etc. Thus instead of treating irregular waves as a hypothetical regular wave train (as in methods A and B) the essential spectral character of a random sea is preserved.

4.0 WAVE MEASUREMENT

Practical methods of acquiring information on the statistics of waves for engineering purposes depend on observing the change in elevation of the surface, or the velocity or pressure at depths smaller than the lengths of the wave components of interest.

4.1 Surface Elevation Methods

The most common methods for acquiring information on the change of surface elevation at a point are resistance, capacitance or transmission line wave gauges. In each case the sensing element or wave staff is installed vertically through the air/water interface and extending above and below it to the limits of its expected excursions. Resistance and capacitance staffs are generally taut wires or slender rods, in which the changes in the elevation of the (conductive) water affect the resistance or capacitance of the staff which is an element of a suitable electric circuit. Transmission line gauges are essentially radio wave guides consisting of a perforated pipe in which the rising and falling water alters the transmission path and so modulates the frequency of a radio frequency oscillator.

The principal advantages of resistance and capacitance staffs are low cost and good spatial resolution. The principal disadvantages are high susceptability to meniscus errors caused by fouling and to damage by floating debris and ice. The transmission line tube largely avoids these disadvantages at the expense of poorer spatial resolution and higher cost.

4.2 Accelerometer Buoys

In many applications wave climate data is needed where no suitable structure to support a wave staff exists or is practicable.In these circumstances a moored accelerometer buoy provides a reliable and economic method of acquiring the necessary data. These buoys contain an accelerometer suitably supported within the buoy so that it remains vertical (or nearly so) as the buoy heaves. The buoy is moored with sufficient scope so that its vertical motion approximates that of the surface. The double integral of the time history of the buoy's

acceleration, corresponding to changes in surface elevation, is transmitted to shore or recorded on board.

4.3 Pressure

Many engineering applications are relatively unconcerned about the shorter (higher frequency) wind waves and instead focus attention on the larger (and long) waves near the peak of the spectrum. In these cases a record of the pressure beneath the surface may provide the most economic solution. As discussed earlier, the magnitude of the pressure disturbance associated with any particular wavelength diminishes rapidly with the ratio of wavelength to probe depth (L/z), so that an appropriate pressure response factor (K_p) must be applied to the measured spectrum in order to recover the equivalent spectrum of surface elevation. Ideally, the pressure port of the instrument should be mounted flush with the bottom but if the water depth (d) is such that $L_{min}/d < 2$ (where L_{min} is the wavelength of the shortest wave desired) then it will be necessary to mount the pressure port above the bottom to avoid burying the desired signal in measurement noise. When this is done care must be taken in the design of the pressure port to minimize contamination of the pressure signal by the flow around the port (Cavaleri 1980).

For many applications ($H/L < 0.05$) the pressure response factor given by small amplitude wave theory is adequate:

$$K_p = \frac{\cosh k(d + z)}{\cosh kd} \tag{37}$$

In deep water ($L_{max}/d < 2$) the pressure response factor simplifies to

$$K_p = e^{kz} \tag{38}$$

For monochromatic waves, a subsurface wave pressure head fluctuation, H_p, can be related to the surface wave height, H by

$$H = \frac{H_p}{K_p} \tag{39}$$

To account for observed deviations from Equation 39, an empirical correction factor, N, has been introduced by many investigators (Cavaleri 1980, Grace 1978, Tubman and Suhayda 1976, Draper 1957) as in:

$$H = \frac{N\, H_p}{K_p} \tag{40}$$

for regular waves, or

$$(\rho g)^2\, \Phi_s(f) = \left[\frac{N(f)}{K_p(f)}\right]^2 \Phi_p(f) \tag{41}$$

for irregular waves

where $\Phi_s(f)$ = surface wave variance spectral density
$\Phi_p(f)$ = subsurface pressure variance spectral density

Other investigators (Forristall 1982, Esteva and Harris 1970, Simpson 1969) have found linear theory to be adequate (N = 1.0). In any case the correction usually will not alter the wave height by more than 10 percent.

Pressure (wave) recorders are often an appropriate wave measuring technique solution in harbours or shipping channels where buoys and wave staffs are hazardous or vulnerable. Their main disadvantage is their poor response to short waves, but this can be turned to advantage to eliminate "wind wave noise" when information is required on long shallow water waves such as seiches, tides and surges. In fact additional filtering is often applied to reduce the demands on data reduction when long period motions are of interest. Caution should be taken in using mechanical filtering for this purpose as is done in conventional tide gauges (Noye 1968, 1972).

4.4 Other Methods

The methods given above have long held a secure place in engineering practice where the emphasis is on local wave climatology, i.e., long term measurements in one or a few chosen spots. Many of the more modern methods have been devised for remote sensing and are particularly well suited to obtaining good areal coverage at a few chosen times. A short list of other methods is given here with appropriate references: radar altimetry (Barnett and Wilkerson 1967); laser altimetry (McClain et al. 1982, Tsai and Gardner 1982); stereo photogrammetry (Cote et al. 1960 and Holthuijsen 1981); synthetic aperature radar (Alpers et al.1981); surface contour radar (Kenney et al. 1979); scanning-beam microwave radar (Jackson et al. 1985); shipboard radar (Young et al. 1985) shore based high frequency radar (Barrick 1972, Teague et al. 1977); optical slope distributions (Irani et al. 1981).

5.0 MEASUREMENT OF WAVE DIRECTION

The measurement of wave direction requires greater instrumental complexity (and hence cost) than does the measurement of wave height. For this reason a climatology of heights (and periods) is often

obtained by measurement and the corresponding distributions of wave direction inferred from the wind climatology. Differences in wave and wind-sea direction can be quite large in fetch limited situations (Donelan et al. 1985) and the effectiveness of some structures (e.g., breakwaters) depends sensitively on wave direction. Thus the additional effort of acquiring a climatology of directions as well as heights and periods may in some instances be justified.

5.1 Arrays of Wave Staffs

Estimates of the directional properties of waves may be deduced from simultaneous recordings from several wave staffs or pressure sensors suitably arranged in the same general area. Barber (1963) has described the method of analysis and Munk et al. (1963) have applied the method to a sparse array of pressure recorders for examining the properties of long swell. An excellent analysis of the design and properties of such arrays is given by Davis and Regier (1977). High resolution directional spectra can be obtained from multi-element arrays (Donelan et al. 1985), but engineering studies generally require information on only the lowest few moments of the directional distribution (often mean direction and root-mean-square spread are sufficient) and therefore cannot justify the considerable cost and expenditure of time and effort required to maintain and analyse multi-element arrays. On the other hand, three wave staffs (or pressure sensors) arranged at three corners of a square of suitable size (depending on the wavelengths of interest) will often yield sufficient wave climatological information (spectra, direction and spread) for engineering purposes and may reap substantial rewards in tighter design and hence lower construction costs.

5.2 Pitch-Roll-Heave Buoys

Perhaps the commonest method of estimating the directional spectrum is by the use of moored buoys containing sensors that respond to heave, pitch and roll (Longuet-Higgins et al. 1963). Such buoys are now commercially available and often come equipped with analysis software so that the desired engineering information from any episode of wave recording is at hand almost immediately from radio or satellite transmission of the analysed data or soon after recovery of onboard recordings.

The basic information sensed by the buoy includes buoy slope in two orthogonal earth-referenced directions and surface elevation (double integral of vertical acceleration). Often the mooring is designed to reduce the likelihood of capsize by providing an erecting force. This reduces the buoy's response to surface slope, but, provided the effect is the same in both orthogonal horizontal directions, the buoy's direction sensing fidelity is not affected. Thus care should be taken to ensure the symmetry of mooring, bridles, etc. The use of such moored directional buoys in areas of strong (>40 cm/s) current is not recommended.

The analysis of the information obtained from "pitch-roll" buoys is given by Longuet-Higgins et al. (1963).

5.3 Pressure-Velocity Sensors

In cases where it is inconvenient to install buoys or wave staffs at the surface a third method, using submerged sensors, often finds favour. The simplest arrangement (Nagata 1964) employs a pressure sensor and two current meters arranged to yield two horizontal orthogonal components. Apart from depth response factors, which degrade the signals from short waves, these pressure-velocity combinations yield equivalent information to pitch-roll-heave buoys.

Two advantages of this method are: (1) the sensors are submerged and hence less subject to damage due to ships, ice, etc.; (2) observed velocities that are incoherent with the pressure signal are due to currents and not waves. These currents are themselves useful in design specifications.

6.0 WAVE STATISTICS

The variability of wave heights is best regarded in a statistical sense as a two-scale process. Within a given storm or wave record wave heights vary considerably, but if conditions are quasi-steady during the storm then the statistical distribution of wave heights can be well-modelled by certain distributions that depend on average properties of the particular sea state. This is the short term wave height distribution. When designing coastal structures, one is also interested in wave conditions over the life of the structure. A much longer time scale associated with the frequency of storms affects the average properties of the wave field, the statistical description of which constitutes a wave "climate". This is the long term wave height distribution.

Clearly these aspects of wave variability depend on the wind, in particular its strength and temporal behaviour. In coastal areas the direction of the wind, topography and bathymetry are also important factors in determining the distribution of wave heights.

6.1 Short Term (Intra-Storm) Height and Period Distributions

The vast majority of observations of changes in surface elevation of a wind-driven sea are in the form of time series of elevation η (or subsurface pressure) at a point. A great deal of success in describing the statistical properties of the surface elevation starts from

the assumption that these arise through the independent propagation of a spectrum of waves of various wavelengths. If the components are assumed to be statistically independent then the distribution of the surface elevation variations, η would be Gaussian:

$$p(\eta) = (2\pi m_0)^{-1/2} \exp\{-\frac{\eta^2}{2 m_0}\} \tag{42}$$

where m_r are the moments of the frequency spectrum $\Phi(f)$ of η:

$$m_r = \int_0^\infty f^r \Phi(f)\, df \tag{43}$$

The zeroth moment

$$m_0 = \sigma^2 = \int_0^\infty \Phi(f)\, df = \overline{\eta^2} = \lim_{T\to\infty} \frac{1}{T} \int_0^T \eta^2\, dt \tag{44}$$

is the variance of surface elevation.

The Gaussian assumption appears to be quite closely satisfied for large natural waves and has been applied successfully as early as 1953 (St. Denis and Pierson) to calculate the motion of ships in a confused sea. Generally speaking the Gaussian assumption is valid in the majority of engineering applications where one is interested in waves near the spectral peak and not in the smaller scale waves at higher frequencies.

The envelope of a Gaussian process has a Rayleigh distribution and if the spectrum is sufficiently narrow (in practice this is generally so) the crest to (preceeding with intervening zero crossing) trough height may be identified with the double amplitude of the envelope. Thus:

$$p(H) = \frac{H}{4\sigma^2} \exp\left\{-\frac{H^2}{8\sigma^2}\right\} \tag{45}$$

or in terms of the normalized height

$$h = \frac{H}{m_0^{1/2}} \tag{46}$$

giving

$$p(h) = \frac{h}{4} \exp\left\{-\frac{h^2}{8}\right\} \tag{47}$$

The probability of exceedance of a given wave height H_+, the cumulative probability, is the integral of (45) from H_+ to ∞

$$P(H_+) = \int_{H_+}^{\infty} p(H)\, dH = \exp\left\{-\frac{H_+^2}{8\sigma^2}\right\} \tag{48}$$

or $$P(h_+) = \exp\left\{-\frac{h_+^2}{8}\right\} \tag{49}$$

These probabilities are graphed in Figure 24.

If one wants to know the average height (or height squared - relevant to force calculations) of waves exceeding h_+, these may be readily computed from (45) and (48)

$$\overline{h_+^n} = \frac{\int_{h_+}^{\infty} h^n\, p(h)dh}{P(h_+)} \tag{50}$$

where n is the power of height whose average is desired. These functions (47), (48) and (50 with n = 1 & 2) are listed in Table 1 for several commonly used reference heights.

Calculation of wave forces on structures requires information on periods associated with wave heights as well as the heights themselves. The joint distribution of heights and periods (Longuet-Higgins 1983) is given by:

$$p(h,\tau) = \frac{h^2}{2\pi^{1/2}\nu[1+(1+\nu^2)^{-1/2}]\tau^2} \exp\{-\frac{h^2}{8}[1+(1-\frac{1}{\tau})^2/\nu^2]\} \quad (51)$$

where $$\tau = \frac{T\, m_1}{m_0} \quad (52)$$

and the spectral width ν is

$$\nu = (\frac{m_0 m_2}{m_1^2} - 1)^{1/2} \quad (53)$$

The theoretical distribution (51) is shown in Figure 25 for two values of the spectral width, ν. The spectral width may be determined directly from observed spectra or from empirical spectral parameterizations. For example, the wind sea spectra of Donelan et al. (1985), described in Section 7.1, have spectral width $\nu = 0.42$, almost independent of wave age (Table 2). For swell, on the other hand, the spectral width is considerably less and the value $\nu = 0.1$ may be taken as typical.

Integration of (51) over appropriate regions of the h,τ plane yields the desired average heights:

$$h_q = q^{-1} \int_{h_+}^{\infty} \int_0^{\infty} hp(h,\tau)\, d\tau\, dh \quad (54)$$

where h_+ is defined implicitly by the cumulative probability function

$$P(h_+) = \int_{h_+}^{\infty} \int_{0}^{\infty} p(h,\tau)\, d\tau\, dh = q \qquad (55)$$

For example, the significant height (average height of highest 1/3 of waves) is given by (54) and (55) with q = 1/3.

The most probable (mode) period associated with a given height, h is τ_m

$$\tau_m = .2 \{1 + (1 + 32\, \nu^2/h^2)^{1/2}\}^{-1} \qquad (56)$$

This is graphed (dashed curve) in Figure 25 and listed in Table 1.

The probability density of τ (regardless of h) is:

$$p(\tau) = \{\nu\tau^2\, [1 + (1 + \nu^2)^{-1/2}][1 + (1 - \tfrac{1}{\tau})^2 \nu^{-2}]^{3/2}\}^{-1} \qquad (57)$$

and is graphed in Figure 26 for two values of the spectral width parameter, ν.

The expected height of the highest wave in a sample of N waves is given by (Longuet-Higgins 1952)

$$E(h_{max}) = \int_0^{\infty} [1 - \{1 - P(h)\}^N]\, dh \qquad (58)$$

where E denotes "expected value of".

For the Rayleigh distribution (narrow frequency band waves) Longuet-Higgins showed that

$$E(h_{max}) = (8 \ln N)^{1/2} + \gamma_E (\tfrac{1}{2} \ln N)^{-1/2} \qquad (59)$$

where γ_E = Euler's constant = 0.5772. The approximation of Equation 59 is within 1.5% of the exact value for N = 20 and quickly improves with increasing N.

Another useful estimate for engineering purposes (Ochi 1973) is the extreme value of h that has a certain probability (q 1) of being exceeded in N waves. Since q*N is the number of waves that exceed h_q on average, then the expected value of h_q is given by:

$$E(h_q) = (8 \ln q^{-1})^{1/2} + \gamma_E(\frac{1}{2} \ln q^{-1})^{-1/2} \quad (60)$$

The statistical estimates are based on assumed knowledge of certain moments of the distribution. In fact all that is ever available are estimates of these moments, so that error bands are associated with all the above calculations. See Section 7.3.

6.2 Probability Distribution of Run Length

Although the average statistical properties of waves conform well with a random model, there is a tendency for high waves to appear in groups (Rye 1982; Nolte and Hsu 1973). The grouping of high waves is significant in many engineering problems where structures or vessels may be excited near their resonant frequencies and in coastal problems such as the stability of breakwaters. One useful index of grouping is the probability distribution of run length or the likelihood of observing a given number of consecutive waves exceeding a chosen height. Kimura (1980) has developed a theory for the probability distribution of run length based on the Rayleigh distribution of wave height and requiring the correlation coefficient between pairs of adjacent heights in a record. Kimura's theory has also been summarized by Goda (1985).

Ewing (1973) has obtained an approximate empirical relationship between mean length $\bar{\ell}$ of runs of waves above a chosen (normalized) height, h_c and Goda's (1970) spectral peakedness parameter, Q_p.

$$\bar{\ell}(h_c) = \sqrt{2}\, Q_p\, h_c^{-1} \tag{61}$$

and

$$Q_p = 2\, m_0^{-2} \int_0^\infty f\Phi^2(f)df \tag{62}$$

The values of Q_p computed from the wind sea spectrum (Equation 64) for various wave ages are given in Table 2.

6.3 Wave Statistics in Shoaling Water

A great deal of theoretical and experimental work has been done on the statistics of wind waves in deep water and the results are summarized in the previous section. However, in many applications the engineer requires estimates of probability of occurrence of waves of various heights and periods in shallow or shoaling water. Various attempts to address wave statistics in shoaling water have been made (Goda 1975, 1985; Thompson and Vincent 1985).

Figure 27 from Thompson and Vincent (1985) allows the prediction of H_s/H_{m_0} as a function of d/gT_p^2 and the significant wave steepness, ε defined as

$$\varepsilon = \frac{H_{m_0}}{4L} \tag{63}$$

H_{m_0} and L can be calculated from Equations 35 and 6 (or 8), H_s can be obtained from Figure 27 (use the "Average" curve) and, then, the approximate distribution of wave heights may be determined from Table 1 (e.g., $\bar{H}_{.01} = 1.67\, \bar{H}_s$) or from Equation 50. These calculations assume a Rayleigh distribution of wave heights but the wave height distribution may be truncated by wave breaking (individual wave heights are assumed to be limited to the same degree as monochromatic waves as shown in

Figure 22). This method also assumes that refraction and diffraction effects are negligible.

When wave conditions are quasi-steady and the combination of beach slope and propagation distance is sufficiently small, the wave period at the peak of the variance spectrum can be assumed to be relatively constant (change of less than 10 percent) from deep to shallow water (Vincent 1984).

6.4 Long Term Distribution of Extremes

There are two basic approaches to estimating extreme waves: (1) From records of wave statistics construct an appropriate distribution (e.g., Gumbel, Weibull) of maxima (Fisher and Tippet 1928) and from this distribution infer the required extremes. (2) From records of wind statistics, construct an appropriate distribution of worst storms and from this distribution infer the required extreme storms. Then apply these storms in a wind-wave hindcast model to determine the extreme sea states during the desired forecast period. The extreme sea states may then be used to deduce extreme heights and the probability of exceedance of these heights using the statistical models described in Section 6.1.

The first method is in common use but the second offers several advantages over the first: (a) A long history of wave climatology is generally not available in most areas, whereas long term meteorological records are. The estimation of extremes appropriate to times much longer than the available record is fraught with error. Thus a much better estimate of extremes in meteorological conditions is possible than of extremes in the wave heights deduced directly from the wave climatology. (b) Local effects such as fetch limits, bottom topography causing refraction and limiting wave heights and lengths are not included in the first method whereas in the second, a good hindcast model will incorporate all these effects and produce a sea state

appropriate to the extreme storms. Thus the second method is highly recommended.

7.0 ANALYSIS OF WAVE RECORDS AND PRESENTATION OF WAVE DATA

7.1 Spectral Analysis

The systematic analysis of wind sea spectra has its origin in the work of Kitaigorodskii (1962). Since then, various parametric descriptions of observed wave spectra have been proposed. Pierson and Moskowitz (1964) proposed a spectral form on the basis of observations of "fully developed" waves in deep water and Hasselmann et al. (1973) extended the concept to include fetch limited waves in earlier stages of development. Bouws et al. (1985) have extended this work to include depth-limited conditions. Donelan et al. (1985) have proposed a spectral form that includes fetch and duration limited cases in deep water in which the waves and wind need not be colinear. The spectral parameters are related to the wave age W (ratio of wave celerity at the spectral peak to the wind speed component in the direction of travel of the peak waves) and in the limit of full development (W = 1.2) their spectral form approaches the Pierson-Moskowitz form. The spectral representation due to Donelan et al. (1985) is derived from data in the wave age range $0.2 < W < 1.2$ and is given by:

$$\Phi(f) = \alpha g^2 (2\pi)^{-4} f^{-4} f_p^{-1} \exp\left\{-\left(\frac{f_p}{f}\right)^4\right\} \gamma \exp\left\{-\frac{(f - f_p)^2}{2\mu^2 f_p^2}\right\} \quad (64)$$

where $\alpha = 0.006\ W^{-0.55}$ (65)

$\mu = 0.08\ (1 + 4\ W^3)$ (66)

$$\gamma = \begin{cases} 1.7 - 2.6 \ln W & ; \quad 0.2 < W < 1 \\ 1.7 & ; \quad 1 < W < 1.2 \end{cases} \tag{67}$$

and f is the cyclic frequency and f_p its value at the spectral maximum. The spectral parameters (α, μ, γ) are functions of the wave age W only. Spectra from Equation 64 for a 10 m/s wind speed and various fetches are shown in Figure 28, and for a 100 km fetch and various wind speeds in Figure 29.

Wind waves are not long-crested but, rather, are distributed about the wind direction with appreciable angular spread. Empirical directional spectra have been given by several researchers including Mitsuyasu et al. (1975), Hasselmann et al. (1980) and Donelan et al. (1985). The directional spectrum or frequency-direction distribution as given by (Donelan et al. 1985) is:

$$F(f, \theta) = \frac{1}{2} \Phi (f) \beta \operatorname{sech}^2 \beta \{\theta - \bar{\theta}(f)\} \tag{68}$$

where $\bar{\theta}(f)$ is the mean wave direction and β, the spreading parameter, is given by:

$$\beta = \begin{cases} 2.61 \left(\frac{f}{f_p}\right)^{+1.3} & ; \quad 0.56 < \frac{f}{f_p} < 0.95 \\ 2.28 \left(\frac{f}{f_p}\right)^{-1.3} & ; \quad 0.95 < \frac{f}{f_p} < 1.6 \\ 1.24 & ; \quad \text{otherwise} \end{cases} \tag{69}$$

The (normalized) shape of the directional distribution (Donelan et al. 1985) is given in Figure 30.

7.2 Sampling Variability of Spectral Estimates

Spectral analysis of a wave record of finite duration leads to a statistical estimate of the true spectrum of the process in the same sense that an average of a sample of random data is an estimate of the true but unknown first moment of the probability density function associated with the sample. The wave record is a (generally short) sample drawn from a much larger population and as such can yield only an estimate of the underlying spectrum of the process. The question is, how accurate is the estimate of the true but unknown spectrum? The simplest model of the statistical behaviour of waves that yields reliable answers to this question is that of a stationary Gaussian process. Although deficient in some respects (e.g., surface is free of skewness, i.e. symmetrical about the mean water level) the model permits the calculation of theoretical confidence limits on spectra which are in excellent accord with observations (Donelan and Pierson 1983).

The spectral estimates, computed from a wave record, are chi-square distributed with d_f degrees of freedom. The number of degrees of freedom, d_f associated with each estimate depends on the length of the record in seconds, t_R, and the frequency bandwidth of the estimate, Δf, where

$$d_f = 2 \Delta f \, t_R \tag{70}$$

Normally fast Fourier transform (FFT) methods are used to obtain a large number of elemental spectral estimates which are then averaged in bands of equal spectral width, Δf.

Once the value of d_f has been established, chi-square tables (e.g., Abramowitz and Stegan 1965) will yield the confidence limits on the spectral estimates.

Multiplicative factors corresponding to 95 percent and 5 percent confidence limits (enclosing a 90 percent confidence band) and to 90 percent and 10 percent confidence limits are given in Table 3 for various values of d_f. For d_f larger than 30 the approximations given by Blackman and Tukey (1958) are given.

The confidence bands decrease quickly at first with increasing degrees of freedom and then more slowly. So that while it is good practice to obtain long enough records so that d_f is large, a value of 30 is a reasonable compromise. Much larger values generally can be obtained only at the expense of over-smoothing of the spectra or accepting non-stationary data. With 30 degrees of freedom the spectrum is known to within a factor of 2 at the 80 percent confidence level. That is, eight times out of ten the true spectrum will be within the 10 percent and 90 percent confidence limits. Increasing the number of degrees of freedom to 90, by tripling the record length or widening the smoothing window so that Equation 70 yields 90, narrows the 80 percent confidence bands to a factor of 1.48.

7.3 Confidence Limits on Variance and Characteristic Height

The estimation of the total variance of the record, σ^2 $(=m_0)$ leading to such estimates as the characteristic height, $H_{m_0} = 4\sigma$ is subject to similar inaccuracies as in 7.2. Since the variance is derived from the entire spectrum, the total degrees of freedom, D_f associated with the variance is larger than the degrees of freedom, d_f associated with each spectral estimate. Donelan and Pierson (1983) describe a method to calculate D_f from a spectrum. The confidence limits on the variance for various values of D_f are given in Table 3. The limits on heights (characteristic height, mean height, etc.) are given by the square root of the multiplicative factors in Table 3.

For wind seas (very little swell) Skafel and Donelan (1983) give the following approximation to the calculation of D_f:

$$D_f \approx 0.86\, N_p \qquad (71)$$

where N_p is the number of peak periods, T_p in the record: $N_p = t_R/T_p$. Figure 31 shows the confidence limits corresponding to Equation 71.

7.4 Confidence Limits on Peak Frequency

Within the confidence limits of discrete spectral estimates the estimated spectral values differ from the true values. In some cases the estimated spectral value at a frequency different from the true peak may be larger than the estimated value at the true peak frequency; accordingly, the estimated peak frequency may be in error by an amount which depends on the confidence limits on the spectrum and the shape of the spectrum. Clearly for given confidence limits a narrow spectrum will be subject to less error than a broad spectrum.

The number of degrees of freedom can be increased by broadening the bandwidth Δf of the averaged bands, however this reduces the possible resolution of the peak frequency. This reduction in resolution may be offset by assigning the peak frequency to the weighted (by spectral estimate) mean of the three spectral bands at and on either side of the highest band.

In Table 4 are summarized the coefficients of variation (ratio of standard deviation to mean) and bias of measured peak frequency for various values of the spectral peakedness parameter, Q_p, bandwidth, Δf and degrees of freedom, d_f. The spectral shape (Equation 64) corresponds to wind-seas of various wave ages. This table has been prepared by Monte Carlo simulation in which the estimated peak frequency is determined from the centroid of the three estimates at and about the estimated peak, as described above. A similar method was applied by Günther (1981) to the JONSWAP spectrum.

7.5 Zero Crossing Method

The spectral methods described above are recommended for engineering design. However, they require considerable machine calculation and there are occasions when a hand graphical technique is useful in providing quick preliminary answers. The so-called "zero crossing method" developed by Tucker (1963) is suitable for this purpose and is described below. The method is based on the assumption of a Rayleigh distribution of wave heights and it simplifies a wave record (such as Figure 32) so that it may be summarized by only two parameters, a wave height and a wave period. The steps in this method are listed below. The square bracketed figures refer to the record in Figure 32.

1. Sketch the mean water level as closely as possible.
2. Count the number of crests - N_C [10].
3. Count the number of zero-up-crossings - N_Z when the record crosses the mean water level in an upward direction [7].
4. The average crest period, $\bar{T}_C$ and the average zero-up-crossing period, $\bar{T}_Z$, may be calculated as

$$\bar{T}_C = \frac{t_R}{N_C} \quad \text{and} \quad \bar{T}_Z = \frac{t_R}{N_Z} \tag{72}$$

   where t_R is the length of the record in seconds.
5. Determine the values of A, B, C and D, the highest crest, the second highest crest, the lowest trough and the second lowest trough respectively.

From these values two estimates of σ, the root mean square value of water surface displacement (Equation 44) may be obtained as

$$\sigma_{x,1} = (A + C) \cdot \frac{1}{2} \cdot (2\lambda)^{-1/2} [1+.289\lambda^{-1} - .247\lambda^{-2}]^{-1} \quad (73)$$

$$\sigma_{x,2} = (B + D) \cdot \frac{1}{2} \cdot (2\lambda)^{-1/2} [1+.211\lambda^{-1} - .103\lambda^{-2}]^{-1} \quad (74)$$

where σ_x is the value of σ estimated by the zero crossing method and

$$\lambda = \ell n\, N_z \quad (75)$$

From these two estimates of σ the significant wave height may be estimated as

$$H_{x,s} = 2[\sigma_{x,1} + \sigma_{x,2}] \quad (76)$$

This method is only applicable to records with a narrow frequency band.

The zero crossing method yields $H_{x,s}$ and $\bar{T}_z$. The remainder of the distributions of H and T may also be obtained from the record by grouping and analysis of the individual waves. One must be careful of definitions at this point, however, and in a number of studies different wave height definitions are used. The normal definition for wave height, H, is the vertical distance between a wave crest and the preceding trough (Figure 32) where crest and trough are defined as maxima and minima of the record. The second definition sometimes used in connection with the zero crossing method is zero crossing wave height, H_z. This is defined as the vertical distance from the maximum crest between a zero up crossing and the subsequent zero down crossing to the minimum trough between the same zero up crossing and the preceding zero down crossing (Figure 32). This second definition removes all the small wavelets that do not cross the mean water level. A careful distinction must be made, for instance, between H_s and $\bar{H}_{z,s}$, $H_{0.1}$ and $\bar{H}_{z,0.1}$ where

the first of each pair refers to the normal definition of wave height while the second uses the zero crossing wave heights H_z.

Goda (1977) provides estimates of the sampling variability of heights and periods determined by the zero-crossing method. The estimates of heights and periods are assumed to be normally distributed about the mean, so that given the coefficient of variability (ratio of standard deviation to mean) the probability that the true height (or period) lies within a certain range about the mean is immediately available from tables of the normal distribution. From his figures the coefficient of variation of significant height, C_{H_s} and of average period, C_T are related to the number of waves analyzed, N_z in the following way:

$$C_{H_s} = 0.71\ N_z^{-0.55} \tag{77}$$

$$C_T = 0.44\ N_z^{-0.51} \tag{78}$$

The coefficient of variation of other height and period parameters may be obtained from Goda's (1985) figures.

7.6 Directional Spectral Analysis

The most common method of obtaining directional wave information for engineering purposes has been by the use of pitch-roll buoys. The method of analysis (direct Fourier transform method) is given by Longuet-Higgins et al. (1963).

Where directional resolution of better than ±30° is required, the direct Fourier transform method may not be adequate. Finer directional resolution may be achieved with "Maximum Likelihood Methods", which strive to minimize the variance between the true spectrum and the estimate, subject to certain constraints. A comprehensive description

of these methods is given by Capon et al. (1967), Capon (1969), Long and Hasselmann (1979) and Isobe et al. (1984). The sampling variability of estimates of wave direction is discussed by Borgman et al. (1982) and by Kuik and Van Vledder (1984).

8.0 WAVE PREDICTION

8.1 General

Wave forecasting refers to the prediction of wave conditions in the future; wave hindcasting is the estimation of past wave conditions from past weather records. Wave prediction is of fundamental importance to the coastal engineer because measured wave data sufficient for engineering design is seldom available at any given location. Basically, wave conditions can be considered to be a function of wind velocity, duration of wind, fetch, depth of water and wave decay rates. A special case, known as fully arisen sea (FAS), exists when the wave conditions depend only on the wind speed because there is no net wave decay and the other variables are sufficiently large that they have no effect; for wind speeds of engineering interest, FAS conditions occur primarily in the oceans.

Simplified wave prediction models yield estimates of a characteristic wave height (or energy) and period. Usually the dominant wave direction is assumed coincident with the wind. Most of these simplified models can be used with an empirical wave spectral shape to provide an estimate of the wave spectral characteristics (assuming no wave decay or incident swell). The two most widely used models are the Sverdrup-Munk-Bretschneider (SMB) model (Sverdrup and Munk 1947, Bretschneider 1958) and the so-called JONSWAP model (Hasselmann et al. 1973). Both use the wind speed at a 10 m height above the water level, hereafter referred to as U_{10}, as the main input parameter.

8.2 Estimating Wind Speed

The greatest source of error in wave prediction involves the estimation of wind speed. The best estimate of wind speed is an over-water wind speed measurement at the location of interest. If the wind is not measured at the 10 m elevation, the wind speed must be adjusted. The simple approximation

$$U_{10} = U_z \left(\frac{10}{z}\right)^{1/7} \tag{79}$$

can be used if the anemometer's elevation, z in metres is less than 20 m.

Most engineering calculations of waves are concerned with quite strong winds so that the atmospheric boundary layer is nearly neutrally stratified; i.e., the stabilizing or destabilizing effect of an air-sea temperature difference is nullified by the strong mechanical wind mixing. A useful index of the degree of stratification is the bulk Richardson number, R_b:

$$R_b = \frac{(T_A - T_W)zg}{T_A U_z^2} \tag{80}$$

where T_A, T_W are air (at height z) and water surface temperature in degrees Kelvin.

If $|R_b| < 0.01$ Equation 79 is valid. Otherwise suitable corrections for stability must be made in establishing UN_{10}, i.e., the equivalent neutral stability wind at the 10 m height. It is this wind speed (UN_{10}) which is appropriately applied to the wave prediction formulae to follow. Formulae for calculating UN_{10} are given in Large and Pond (1981), in which a different stability index is used. The

relationship between this stability index and R_b is given by Donelan et al. (1974).

Overwater wind data is usually unavailable so data from nearby sites on land (airports) is often used. Winds over the water are usually stronger than those over the land. A relationship between overwater (U_W) and overland (U_L) wind speeds for the Great Lakes can be found in Resio and Vincent (1977) or the Shore Protection Manual (1984). A detailed comparison of overwater and overland wind measurements in Lake Erie can be found in Phillips and Irbe (1978). If the land station is close to the water (within 500 m) the correction factor for onshore winds can be assumed equal to unity. Typical correction factors for offshore winds of engineering significance are in the range of 1.2 to 1.5.

8.3 Estimating Fetch

Fetch is the open water distance over which the wind blows with reasonably uniform speed and direction. For the JONSWAP and SMB models, fetch is usually estimated as the straight line distance in the direction of the wind to the edge of the wave generating area (coastline, island, shoal or discontinuity in the weather system). For irregular shorelines some form of fetch-averaging can be done. The Shore Protection Manual (1984) recommends extending 9 radials, at 3 degree intervals (i.e., wind direction ±12 degrees) from the point of interest to the upwind fetch boundary and arithmetically averaging the measured lengths.

8.4 JONSWAP Model

The JONSWAP equations (Hasselmann et al. 1973) relating characteristic wave height (H_{m_0}), period of the spectral peak (T_p), fetch (F) and wind duration (t), are

$$H_{m_0} = 0.0016\ g^{-1/2}\ U_{10}\ F^{1/2} \tag{81}$$

$$T_p = 0.286\ g^{-2/3}\ (U_{10}\ F)^{1/3} \tag{82}$$

$$t = 65.6\ (gU_{10})^{-1/3}\ F^{2/3} \tag{83}$$

These equations are valid in deep water ($d/L > 0.5$) for locally generated seas. The relations are given in a nomogram in Figure 33. The nomogram is entered with values of U, F and t. The intersection of U and F will yield one set of values for H_{m_0} and T_p (fetch-limited waves); the intersection of U and t will yield another (duration-limited waves). The smaller of the two sets of values is chosen as the design set.

The JONSWAP equations are presented in dimensionless form in Figures 34 and 35 with adjustments for shallow water effects (Shore Protection Manual 1984). Use of the deepwater wave curve will give the same results as Figure 33 for fetch-limited conditions. For transitional and shallow water depths, assumed to be constant over the fetch, compute the value of gd/U_{10}^2 and use the appropriate curve. The curves labelled maximum wave height (Figure 34) and maximum wave period (Figure 35) indicate full wave growth, meaning that the wave parameters to the right of these curves are not fetch-limited. When using Figures 34 or 35 the storm duration t should be calculated using Equation 83 to check whether the waves are duration-limited. More detailed nomograms for shallow water wave prediction can be found in the Shore Protection Manual (1984).

8.5 Estimating Wave Direction

Until recently, most simple wave prediciton models assumed coincident wind and wave directions ($\theta = 0$ where θ is the angle between wind and wave directions). However, it has been shown that waves with frequencies near the spectral peak can, in non-stationary (Hasselmann et al. 1980) or fetch-limited (Donelan et al. 1985) conditions, travel at off-wind angles. Values of θ up to 50 degrees have been observed in Lake Ontario (Donelan 1980). In fact, if the fetch gradient about the wind direction is large, one can expect the wave direction to be biased towards the longer fetches if the reduced generating force of the lower wind component ($U \cos \theta$) is more than balanced by the longer fetch over which it acts (Donelan 1980).

A relation for the dominant wave energy direction (ψ) versus wind direction (ϕ) in deep water can be determined for any given location (Figure 36). For fetch-limited conditions Donelan et al. (1985) found that the ψ versus θ relation for a point with known fetch distribution F_ψ could be obtained by maximizing the expression

$$\cos \theta \; F_\psi^{0.426} \tag{84}$$

The ψ versus θ relation for point 0 on an elliptical lake is shown in Figure 37.

A simple manual procedure for obtaining the ψ versus θ relation for any point in deep water is given below.

1. Starting in the wind direction and working towards longer fetches, extend radials from the point of interest to the fetch boundary in the upwind direction as far as the fetch continues to increase. Radials should be at some convenient interval depending on the fetch

lengths and the desired resolution. An interval of 3 to 5 degrees would suffice in many applications.

2. Measure the fetch lengths.
3. Compute $\cos\theta\ F_\psi^{0.426}$.
4. The maximum value of the expression $\cos\theta\ F_\psi^{0.426}$ for any particular wind direction gives the corresponding dominant wave direction.

This procedure can easily be computerized. Calculation of wave direction, while not warranted for all wave predictions, may be important in the design of deep water structures, the estimation of wave climates, etc. In shallower and transitional water depths, refraction effects may alter wave directions further.

Knowing the ψ versus θ relation, somewhat improved accuracy in the prediction of H_{m_0} and T_p can be achieved (Bishop 1983) using the equations of Donelan (1980):

$$H_{m_0} = 0.00366\ g^{-0.62}\ (U_{10}\cos\theta)^{1.24}\ F_\psi^{0.38} \tag{85}$$

$$T_p = 0.54\ g^{-0.77}\ (U_{10}\cos\theta)^{0.54}\ F_\psi^{0.23} \tag{86}$$

$$t = 30.1\ g^{-0.23}\ (U_{10}\cos\theta)^{-0.54}\ F_\psi^{0.77} \tag{87}$$

where F_ψ is the fetch in the dominant wave direction. Unless θ is small, the use of F (fetch in the wind direction) rather than F_ψ in these equations will result in poorer accuracy of prediction than the use of the JONSWAP equations.

8.6 Numerical Models

The computation of wave climates, wave spectra and wave directional information is best done using numerical models. For the Great Lakes, a widely used spectral model is that of Resio and Vincent (1977), while the parametric model of Schwab et al. (1983) gives estimates of H_{m_0}, T_p and the dominant wave direction at each grid point. For oceanic conditions the discrete spectral ocean wave models of Pierson et al. (1966), Pierson (1982) and Golding (1985) and the hybrid (parametric wind sea, discrete swell) models of Günther and Rosenthal (1985) and DeVoogt et al. (1985) are commonly used.

REFERENCES

Abernethy, C.L. and Gilbert, G. 1975. Refraction of wave spectra. Hydraulics Research Station, Report INT 117, Wallingford, England.

Abramowitz, M. and Stegun, I. (Editors) 1965. Handbook of mathematical functions. U.S. Dept. of Commerce, National Bureau of Standards. Applied Mathematics Series. 55, 1046 pp.

Airy, G.B. 1845. Tides and Waves. Encyclopedia Metropolitana, 192, 241-396.

Alpers, W.R., Ross, D.B. and Rufenach, C.L. 1981. On the detectability of ocean surface waves by real and synthetic aperature radar. J. Geophys. Res. 86, 6481-6498.

Barber, N.F. 1963. The directional resolving power of an array of wave detectors. Ocean Wave Spectra. Prentice-Hall, Inc., 137-150

Barnett, T.P. and Wilkerson, J.C. 1967. On the generation of ocean wind waves as inferred from airborne radar measurements of fetch-limited spectra. J. Mar. Res. 25, 292-321.

Barrick, D.E. 1972. First-order theory and analysis of MF/HF/VHF scatter from the sea. IEEE Transactions, Antennas Propagation, AP-20 2-10.

Berger, U. and Kohlhase, S. 1976. Mach-reflection as a diffraction problem. Proceedings of 15th Conference on Coastal Engineering, ASCE, Vol. 1, 796-814.

Birkemeier, W.A. and Dalyrmple, R.A. 1975. Nearshore water circulation induced by wind and waves. Proc. Symp. Modelling Technique. ASCE. 1062-1081.

Bishop, C.T. 1983. Comparison of manual wave prediction models. Journal of Waterway, Port, Coastal and Ocean Engineering, American Society of Civil Engineers, Vol. 109, No. 1, 1-17.

Blackman, R.B. and Tukey, J.W. 1958. The measurement of power spectra from the point of view of communications engineering. Dover Publications Inc., 190 p.

Blue, F.L., Jr. and Johnson, J.W. 1949. Diffraction of water waves passing through a breakwater gap. Trans. Amer. Geophysical Union, Vol. 30, No. 5, 705-718.

Borgman, L.E., Hagan, R.L. and Kuik, A.J. 1982. Statistical precision of directional spectrum estimation with data from a tilt-and-roll buoy. In: Topics in Ocean Physics, edited by Osborne, A.R. and Rizzoli, P.M., Noord-Holland, Amsterdam, 418-438.

Bouws, E., Günther, H., Rosenthal, W. and Vincent, C.L. 1985. Similarity of the wind wave spectrum in finite depth water, 1. Spectral Form. J. of Geophysical Research, Vol. 90, No. C1, 975-986.

Brampton, A.H. 1981. A computer method for wave refraction. Hydraulics Research Station, Report IT 172, Wallingford, England.

Brater, E.F. and King, H.W. 1976. Handbook of Hydraulics, Sixth Edition. McGraw-Hill.

Bretschneider, C.L. 1958. Revisions in wave forecasting; deep and shallow water. Proceedings of 6th Conference on Coastal Engineering, American Society of Civil Engineers, New York.

Capon, J., Greenfield, R.J. and Kolker, R.J. 1967. Multidimensional maximum-likelihood processing of a large aperture seismic array. Proceedings IEEE, Vol. 55, 192-211.

Capon, J. 1969. High-resolution frequency wavenumber spectrum analysis. Proc. IEEE, 57, No. 8.

Cavaleri, L. 1980. Wave measurement using pressure transducer. Oceanologica Acta, Vol. 3, 3:339-345.

Chao, Y-Y. 1972. Refraction of ocean surface waves on the continental shelf. Offshore Technology Conference, OTC 1616, I965 - I974.

Chao, Y-Y. and Pierson, W.J. 1972. Experimental studies of the refraction of uniform wave trains and transient wave groups near a straight caustic. J. Geophys. Res., 77, 4545-4554.

Cote, L.J., Davis, J.O., Marks, W., McGough, R.J., Mehr, E., Pierson, W.J. Jr., Ropek, J.F., Stephenson, G. and Vetter R.C. 1960. The directional spectrum of wind-generated sea as determined from data obtained by the stereo wave observation project: Meteor. Pap., New York University, College of Engineering, Vol. 2, no. 6, 88 pp.

Davis, R.E. and Regier, L. 1977. Methods for estimating directional wave spectra from multi-element arrays. J. Mar. Res. 35, 453-477.

Dean, R.G. 1974. Evaluation and development of water wave theories for engineering application. Special Report No. 1, U.S. Army Corps of Engineers, Coastal Engineering Research Center, Ft. Belvoir, Virginia.

DeVoogt, W.J.P. Komen, G.J. and Bruinsma, J. 1985. The KNMI operational wave predicton model GONO. Proc. Symp. Wave Dynamics and Radio Probing of Ocean Surface. Miami, 1981. Plenum Press.

Dobson, R.S. 1967. Some applications of digital computers to hydraulic engineering problems. TR-80, Chapter 2, Department of Civil Engineering, Stanford University, Palo Alto, California.

Donelan, M.A. 1980. Similarity theory applied to the forecasting of wave heights, periods and directions. Proc. Canadian Coastal Conf. 1980. National Research Council Canada, 47-61.

Donelan, M.A. Birch, K.N. and Beesley, D.C. 1974. Generalized profiles of wind speed, temperature and humidity. Internat. Assoc. Great Lakes Res., Conf. Proc. 17, 369-388.

Donelan, M.A. and Pierson, W.J. 1983. The sampling variability of estimates of spectra of wind-generated gravity waves. Journal of Geophysical Research, Vol. 88, No. C7, 4381-4392.

Donelan, M.A., Hamilton, J. and Hui, W.H. 1985. Directional spectra of wind-generated waves. Phil. Trans. R. Soc. Lond. A 315, 509-562.

Dorrestein, R. 1960. Simplified method of determining refraction coefficients for sea waves. J. Geophys. Res., Vol. 65, No. 2, 637-642.

Draper, L.G. 1957. Attenuation of sea waves with depth. La Houille Blanche, Vol. 12, 6: 926-931.

Eckart, C. 1952. The propagation of gravity waves from deep to shallow water. Gravity Waves, Circular No. 521, National Bureau of Standards, Washington, D.C.

Esteva, D. and Harris, L. 1970. Comparison of pressure and staff wave gage records. Proceedings of the 12th Coastal Engineering Conference, American Society of Civil Engineers, 1: 101-116.

Ewing, J. 1973. Mean length of runs of high waves. J. Geophysical Research, Vol. 78, No. 12, 1933-1936.

Fisher, R.A. and Tippet, L.H.C. 1928. Limiting forms of the frequency distribution of the largest or smallest number of a sample. Proc. Camb. Phl. Soc., 24, 180-190.

Forristall, G.Z. 1982. Subsurface wave-measuring systems. In: Measuring Ocean Waves, National Academy Press, Washington, D.C., 194-209.

Goda, Y. 1970. Numerical experiments on wave statistics with spectral simulation. Report of Port and Harbour Research Institute, Vol. 9, No. 3, 3-57.

Goda, Y. 1975. Irregular wave deformation in the surf zone. Coastal Engineering in Japan. Vol. 18, 13-26.

Goda, Y. 1976. Irregular sea waves for the design of harbour structures. Transactions Japan Society of Civil Engineers, Vol. 8, 267-271.

Goda, Y. 1977. Numerical experiments on statistical variability of ocean waves. Report of Port and Harbour Research Institute, Vol. 16, No. 2, 3-26.

Goda, Y. 1985. Random seas and design of maritime structures. University of Tokyo Press, Japan. 323 p.

Goda, Y., Takayama, T. and Suzuki, Y. 1978. Diffraction diagrams for directional random waves. Proceedings of the 16th Conference on Coastal Engineering, American Society of Civil Engineers, 1: 628-650.

Golding, B. 1985. The U.K. meteorological office operational wave model. Proc. Symp. Wave Dynamics and Radio Probing of Ocean Surface. Miami, 1981. Plenum Press.

Grace, R.A. 1978. Surface wave height from pressure records. Coastal Engineering, 2: 55-67.

Günther, H. 1981. A parametric surface wave model and the statistics of the prediction parameters. Edited by Geophysikalisches Institut University of Hamburg, Hamburger Geophysikalische Einzelschriften 55.

Günther, H. and Rosenthal, W. 1985. The hybrid parametrical (HYPA) wave model. Proc. Symp. Wave Dynamics and Radio Probing of the Ocean Surface. Miami, 1981. Plenum Press.

Harms V.W. 1979. Diffraction of water waves by isolated structures. Journal of the Waterway, Port, Coastal and Ocean Division, American Society of Civil Engineers, Vol. 105, WW2:131-147.

Hasselmann, K., Barnett, T.P., Bouws, E., Carlson, H., Cartwright, D.E., Enke, K., Ewing, J.A., Gienapp, H., Hasselmann, D.E., Kruseman, P., Meerburg, A., Muller, P., Olbers, D.J., Richter, K., Sell, W., and Walden, H. 1973. Measurements of wind-wave growth and swell decay during the Joint North Sea Wave Project (JONSWAP). Deut. Hydrogr. Z., Suppl. A, 8, No. 12, 22 pp.

Hasselmann, D.E., Dunckel, M. and Ewing, J.A. 1980. Directional wave spectra observed during JONSWAP 1973. J. Phys. Oceanogr. 10, 1264-1280.

Holthuijsen, L.H. 1981. The directional energy distribution of wind generated waves as inferred from stereophotographic observations of the sea surface. Thesis, Delft University of Technology. Rep. No. 81-2, 193 pp.

Hughes, S.A. 1984. The TMA shallow-water spectrum description and applications. U.S. Army Waterways Experiment Station, Coastal Engineering Research Centre, Technical Report 84-7, Vicksburg, Mississippi.

Irani, G.B., Gotwols, B.L. and Bjerkaas, A.W. 1981. Ocean wave dynamics test: results and interpretations. Rep. No. STD-R-537, The Johns Hopkins University, Applied Physics Laboratory, 202 pp.

Isobe, M., Kondo, K. and Horikawa, K. 1984. Extension of MLM for estimating directional wave spectrum. Proceedings Symposium on Description and Modelling of Directional Seas. Paper No. A-6, 1-15, Technical University of Denmark.

Jackson, F.C., Walton, W.T. and Baker, P.L. 1985. Aircraft and satellite measurement of ocean wave directional spectra using scanning beam microwave radars. J. Geophys. Res. 90, No. C1, 987-1004.

Johnson, J.W. 1952. Generalized wave diffraction diagrams. Proceedings of the 2nd Conference on Coastal Engineering, American Society of Civil Engineers, New York.

Karlsson, T. 1969. Refraction of continuous ocean wave spectra. Proc. ASCE, Vol. 95, No. WW4, pp. 437-448.

Kenney, J.E., Uliana, E.A. and Walsh, E.J. 1979. The surface contour radar, a unique remote sensing instrument. IEEE Trans. Microwave Theory and Techniques, MTT-27, No. 12, 1080-1092.

Kimura, A. 1980. Statistical properties of random wave groups. Proceedings 17th Coastal Engineering Conference, American Society of Civil Engineers, Vol 3, 2955-2973.

Kitaigorodskii, S.A. 1962. Applications of the theory of similarity to the analysis of wind-generated wave motion as a stochastic process. IZV. Akad. Nank SSSR, Ser. Geofiz, 1, 73-80.

Korteweg, D.J. and De Vries, G. 1895. On the change of form of long waves advancing in a rectangular canal, and on a new type of long stationary wave. Philosophical Magazine, Series 5, 39: 422-443.

Kuik, A.J. and van Vledder, G. Ph. 1984. Proposed method for the routine analysis of pitch-roll buoy data. Proceedings Symposium on Description and Modelling of Directional Seas. Paper No. A-5, 1-13, Technical University of Denmark.

Large, W.G. and Pond, S. 1981. Open ocean momentum flux measurements in moderate to strong winds. J. Phys. Oceanog. 11, 324-336.

Long, R.B. and Hasselmann, K. 1979. A variational technique for extracting directional spectra from multi-component wave data. Journal of Physical Oceanography, Vol. 9, No. 2, 373-381.

Longuet-Higgins, M.S. 1952. On the statistical distributions of the heights of sea waves. Journal of Marine Research, Vol. IX, No. 3, 245-266.

Longuet-Higgins, M.S. 1983. On the joint distribution of wave periods and amplitudes in a random wave field. Proc. R. Soc. Lond. A 389, 241-258.

Longuet-Higgins, M.S., Cartwright, D.E. and Smith N.D. 1963. Observations of the directional spectrum of sea waves using the motions of a floating buoy. In: Ocean Wave Spectra, pp. 111-136. Englewood Cliffs, N.J.: Prentice Hall, Inc.

McClain, C.R., Chen, D.T. and Hart, W.D. 1982. On the use of laser profilometry for ocean wave studies. Journal of Geophysical Research, 87, No. C12, 9509-9515.

McCowan, J. 1891. On the solitary wave. Philosophical Magazine, Series 5, 32: 45-58.

Michell, J.H. 1893. On the highest waves in water. Philosophical Magazine, 5th Series, Vol. 36, 430-437.

Mitsuyasu, H., Tasai, F., Suhara, T., Mizumo, S., Ohkuso, M., Honda, T. and Rikiishi, K. 1975. Observations of the directional spectrum of ocean waves using a cloverleaf buoy. J. Phys. Oceanogr., 5, 750-760.

Munk, W.H., Miller, G.R., Snodgrass, F.E. and Barber, N.F. 1963. Directional recording of swell from distant storms. Phil. Trans. R. Soc. Lond. A 255, 505-584.

Nagata, Y. 1964. The statistical properties of orbital wave motions and their application for the measurement of directional wave spectra. Journal of the Oceanographic Society of Japan, Vol. 19, No. 4, 169-191.

Nolte, K.G. and Hsu, F.H. 1973. Statistics of ocean wave groups. 4th Offshore Tech. Conf., No. 1688.

Noye, B.J. 1968. The frequency response of a tide-well. Proc. 3rd Australian Conf. on Hydraulics and Fluid Mechanics, Sydney, 65-71.

Noye, B.J. 1972. On the differential equations for the conventional tide-well system. Bull. Australian Math. Soc., Vol. 7, 251-267.

Ochi, M.K. 1973. On prediction of extreme values. J. Ship Research (March 73) 29-37.

Palmer, R.Q. 1957. Wave refraction plotter. U.S. Army Corps of Engineers, Beach Erosion Board, Vol. 11, Bulletin No. 1, Washington, D.C.

Penny, W.G. and Price, A.T. 1944. Diffraction of sea waves by a breakwater. Artificial Harbors, Technical History No. 26, Sec. 3-D, Directorate of Miscellaneous Weapons Development.

Pierson, W.J. 1972. The loss of two British trawlers - a study in wave refraction. J. Navigation, 25, 291-304.

Pierson, W.J. 1982. The spectral ocean wave model (SOWM). A Northern Hemisphere Computer Model for Specifying and Forecasting Ocean Wave Spectra. David W. Taylor, Naval Ship Research and Development Center. DTNSRDC-82/011.

Pierson, W.J. and Marks, W. 1952. The power spectrum analysis of ocean-wave records. Trans. Amer. Geophys. Union. 33, No. 6, 834-844.

Pierson, W.J. and Moskowitz, L. 1964. A proposed spectral form of fully developed wind seas based on the similarity law of S.A. Kitaigorodskii. Journal of Geophysical Research, Vol. 69, No. 24, 5181-5190.

Pierson, W.J. and Holmes, P. 1965. Irregular wave forces on a pile. Journal of the Waterways and Harbors Division, Proceedings of the American Society of Civil Engineers, Vol. 91, No. WW4, 1-10.

Pierson, W.J., Tick, J. and Baer, L. 1966. Computer based procedures for preparing global wave forecasts and wind field analyses capable of using wave data obtained by a spacecraft. Proc. 6th Naval Hydrodynamics Symp., Publ. ACR-136, Office of Naval Research, Department of the Navy, Washington, D.C.

Phillips, D.W. and Irbe, J.G. 1978. Lake to land comparison of wind, temperature and humidity on Lake Ontario during the International Field Year for the Great Lakes. Report CLI-2-77, Atmospheric Environment Service, Downsview, Ontario.

Resio, D.T. and Vincent C.L. 1977. Estimation of Winds over the Great Lakes. Journal of the Waterway, Port, Coastal and Ocean Division, American Society of Civil Engineers, Vol. 103, WW4, 265-283.

Rye, H. 1982. Ocean wave groups. Dept. Marine Tech., Norwegian Inst. Techn., Report. UR-82-18, 214 p.

Schwab, D.J., Bennett, J.R., Lui, P.C. and Donelan, M.A. 1984. Application of a simple numerical wave prediction model to Lake Erie. J. Geophys. Res., 89, No. C3, 3586-3592.

Shore Protection Manual. 1984. U.S. Army Corps of Engineers, Coastal Engineering Research Center, Vicksburg, Mississippi.

Shuto, N. 1974. Nonlinear long waves in a channel of variable section. Coastal Eng. in Japan. 17, 1-12.

Simpson, J.H. 1969. Observations of the directional characteristics of waves. Geophysical Journal of the Royal Astronomical Society, 17: 92-120.

Skafel, M.G. and Donelan, M.A. 1983. Performance of the CCIW wave direction buoy at ARSLOE. IEEE J. Oceanic Eng. OE-8, No. 4, 221-225.

Sommerfeld, A. 1896. Mathematische Theorie der Diffraktion. Mathematische Annalen 47, 317-374.

St. Denis, M. and Pierson, W.J. 1953. On the motions of ships in confused seas. Trans. Soc. Naval Architects and Marine Engineers, 61, 280-357.

Stokes, G.G. 1847. On the theory of oscillatory waves. Mathematical and Philisophical Papers, Cambridge University Press, London, 1: 314-326.

Sverdrup, H.U. and Munk, W.H. 1947. Wind, sea and swell: Theory of relations for forecasting. Publication No. 601, U.S. Navy Hydrographic Office, Washington, D.C.

Tayfun, M.A., Dalrymple, R.A. and Yang, C.Y. 1976. Random wave-current interactions in water of varying depth. Ocean Engineering, 3, No. 6, 403-420.

Teague, C.C. Tyler, G.L. and Stewart R.H. 1977. Studies of the sea using HF radio scatter. IEEE Journal of Oceanic Engineering, OE-2, No. 1, 12-19.

Thompson, E.F. 1980. Energy spectra in shallow U.S. coastal waters. Technical Paper 80-2, U.S. Army Corps of Engineers, Coastal Engineering Research Center, Fort Belvoir, Virginia.

Thompson, E.F. and Vincent, C.L. 1985. Significant wave height for shallow water design. ASCE. J. Waterway, Port, Coastal and Ocean Engineering, Vol. 111, No. 5, 828-842.

Thornton, E.B. and Guza, R.T. 1982. Energy saturation and phase speeds measured on a natural beach. Journal of Geophysical Research, Vol. 87, C12:9499-9508.

Tsai, B.M. and Gardner, C.S. 1982. Remote sensing of sea state using laser altimeters. Applied Optics, 21, No. 21, 3932-3940.

Tubman, M.W. and Suhayda, J.H. 1976. Wave action and bottom movements in fine sediments. Proceedings of the 15th Coastal Engineering Conference, American Society of Civil Engineers, 2: 1168-1183.

Tucker, M.J. 1963. Analysis of records of sea waves. Proceedings of the Institute of Civil Engineers, Vol. 26, 10: 305-316.

Tucker, M.J., Carr, M.P. and Pitt, E.G. 1983. The effect of an offshore bank in attenuating waves. Coastal Engineering, Vol. 7, 2:133-144.

Vincent, C.L. 1985. Energy saturation of irregular waves during shoaling. Journal of Waterway, Port, Coastal and Ocean Engineering, ASCE, Vol. 111.

Wiegel, R.L. 1962. Diffraction of waves by a semi-infinite breakwater. Journal of the Hydraulics Division, American Society of Civil Engineers, Vol. 88, HY1: 27-44.

Wiegel, R.L. 1964. Oceanographical Engineering. Prentice-Hall, Inc., Englewood Cliffs, New Jersey.

Wilson, W.S. 1966. A method for calculating and plotting surface wave rays. TM-17, U.S. Army Engineering Waterways Experiment Station, Vicksburg, Mississippi.

Young, I., Rosenthal, W. and Ziemer, F. 1985. A three-dimensional analysis of marine radar images for the determination of ocean wave directionality and surface currents. J. Geophys. Res. 90, No. C1. 1061-1067.

TABLE 1

Some Wave Height and Period Statistics

(Heights and Periods are Normalized)

Symbol	Description	Normalized Height	Probability of Exceedance	Root-Mean-Square	Most Probable (normalized) Period	
					$\nu = 0.1$	$\nu = 0.4$
$\bar{h}_{.01}$	average of highest 1% of the waves	6.68	0.004	6.70	1.00	0.97
$h_{.01}$	height, exceeded by 1% of the waves	6.07	0.010			
$\bar{h}_{0.1}$	average of highest 10% of the waves	5.10	0.039	5.14	1.00	0.96
$h_{0.1}$	height exceeded by 10% of the waves	2.96	0.100			
$h_S = \bar{h}_{1/3}$	significant wave height (average height of the highest 1/3 of the waves)	4.01	0.134	4. 0	1.0	0.9
$h_{1/3}$	height exceeded by 1/3 of the waves	2.96	0.333			
$\bar{h} = \bar{h}_{1.0}$	average wave height	2.51	0.456	2.83	0.99	0.85
$h_{0.5}$	median wave height	2.35	0.500			
h_{mode}	most probable wave height	2.00	0.607			

Note: H_{m_0} is an energy-based, rather than statistically-based, wave height descriptor. In deep water H_{m_0} is generally accepted as being equal to Hs.

TABLE 2

Peak Enhancement Parameter, γ
Spectral Width, ν and Peakedness, Q_p
of a model wind sea (Equation 64) for various wave ages, W

W	State of Development	γ	ν	Q_p
1.2	Fully developed	1.70	0.414	1.90
1.0	Increasingly fetch	1.70	0.422	1.95
0.8	Limited	2.28	0.419	2.18
0.6	↓	3.03	0.419	2.51
0.4		4.09	0.418	2.95
0.2		5.89	0.408	3.65

TABLE 3

Confidence Limits on Spectra

Degrees of Freedom d_f or D_f	Multiply smoothed spectral estimates by this factor to get appropriate confidence limit			
	5%	10%	90%	95%
2	0.334	0.434	9.49	19.50
4	0.422	0.514	3.76	5.63
8	0.516	0.599	2.29	2.93
16	0.608	0.680	1.72	2.01
30	0.685	0.745	1.46	1.62
d_f, D_f > 30	$10^{-(d_f-1)^{-1/2}}$	$6.3^{-(d_f-1)^{-1/2}}$	$6.3^{+(d_f-1)^{-1/2}}$	$10^{+(d_f-1)^{-1/2}}$

TABLE 4

Variability of Estimates of Peak Frequency

W	Q_p	$\frac{\Delta f}{f_p}$	d_f	Bias %	Coefficient of Variation %
0.4	2.94	0.05	10	0.2	4.5
			20	0.1	3.4
			40	0.1	2.9
			80	0.0	2.4
			160	0.0	1.9
		0.1	10	0.3	4.4
			20	0.2	2.7
			40	0.2	1.7
			80	0.1	0.8
			160	0.1	0.4
		0.2	10	1.1	2.7
			20	1.0	1.5
			40	1.0	0.9
			80	1.0	0.6
			160	1.0	0.5
0.8	2.18	0.05	10	2.0	8.5
			20	1.5	7.4
			40	1.1	6.5
			80	0.8	5.4
			160	0.6	4.5
		0.1	10	2.4	9.0
			20	1.3	7.3
			40	1.2	6.5
			80	1.1	5.5
			160	1.0	4.5
		0.2	10	4.0	8.9
			20	2.8	5.8
			40	2.4	4.1
			80	2.0	2.2
			160	1.7	0.8
1.2	1.90	0.05	10	4.1	11.2
			20	2.6	9.6
			40	2.2	8.6
			80	1.8	7.3
			160	1.4	5.7
		0.1	10	4.9	12.1
			20	3.2	10.1
			40	2.6	8.6
			80	2.1	7.4
			160	1.8	6.1
		0.2	10	7.1	12.4
			20	5.5	9.1
			40	4.5	7.3
			80	3.6	5.1
			160	2.8	3.9

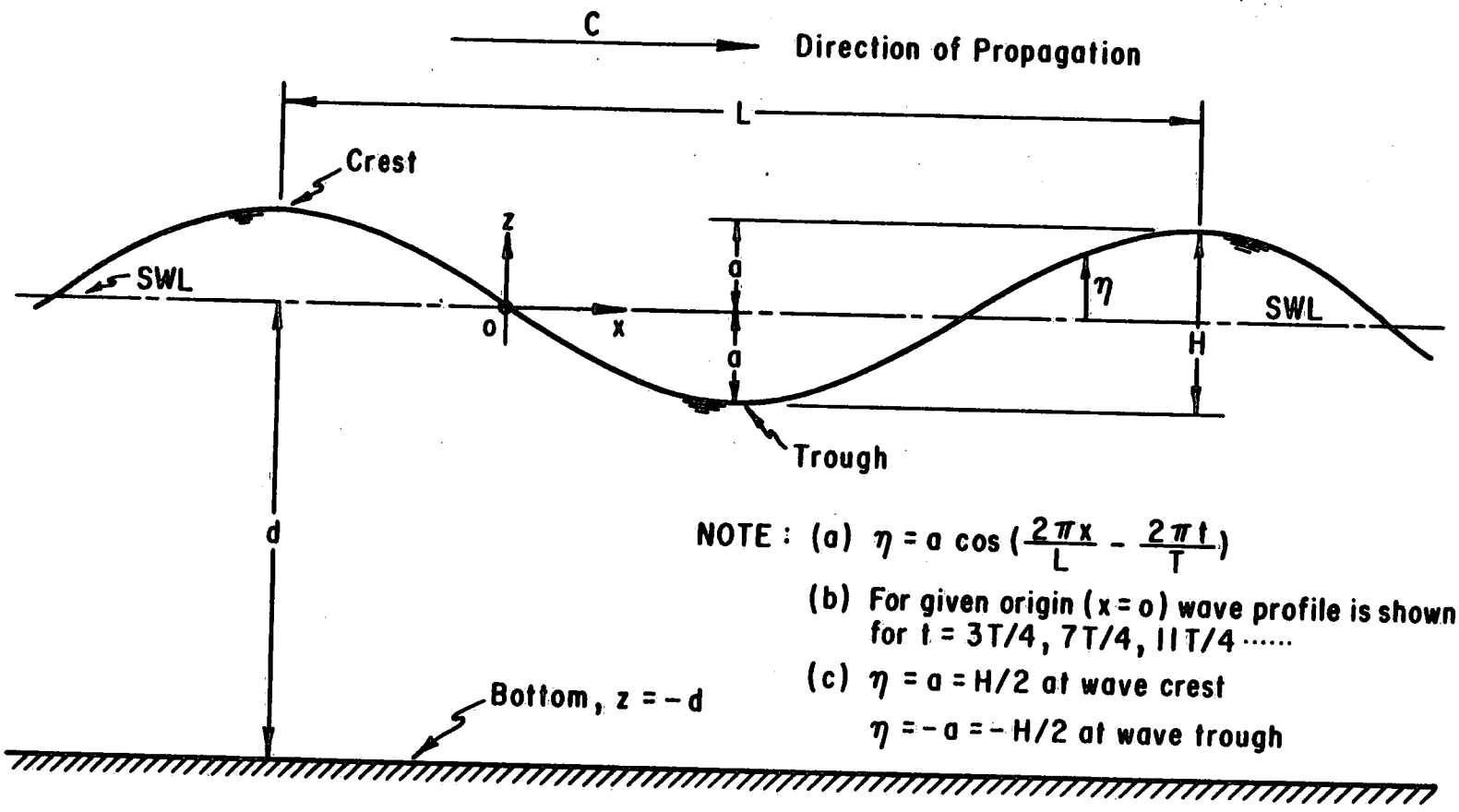

Figure 1. Definition sketch of simple, sinusoidal, progressive wave (Shore Protection Manual 1984).

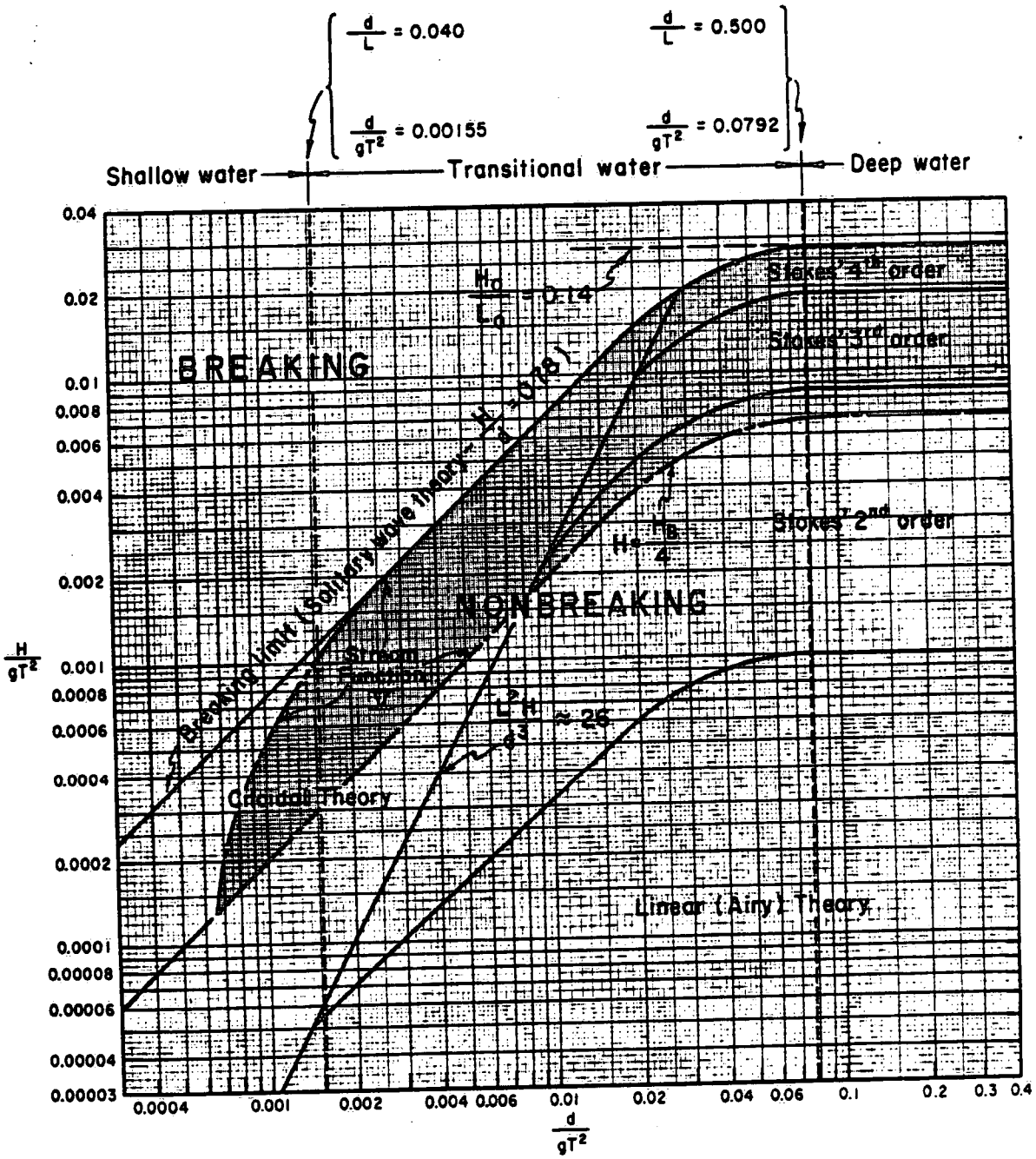

Figure 2. Regions of validity for various wave theories (after Le Méhauté 1969, Shore Protection Manual 1984).

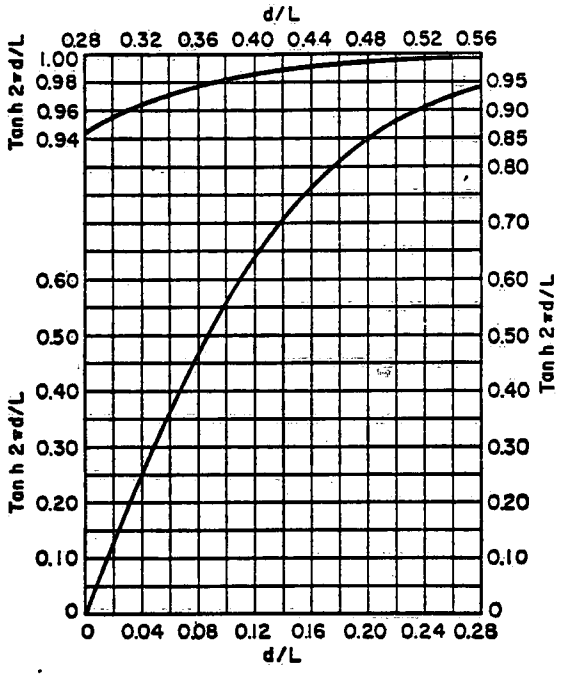

Figure 3. Tanh 2πd/L versus d/L (Brater and King 1976).

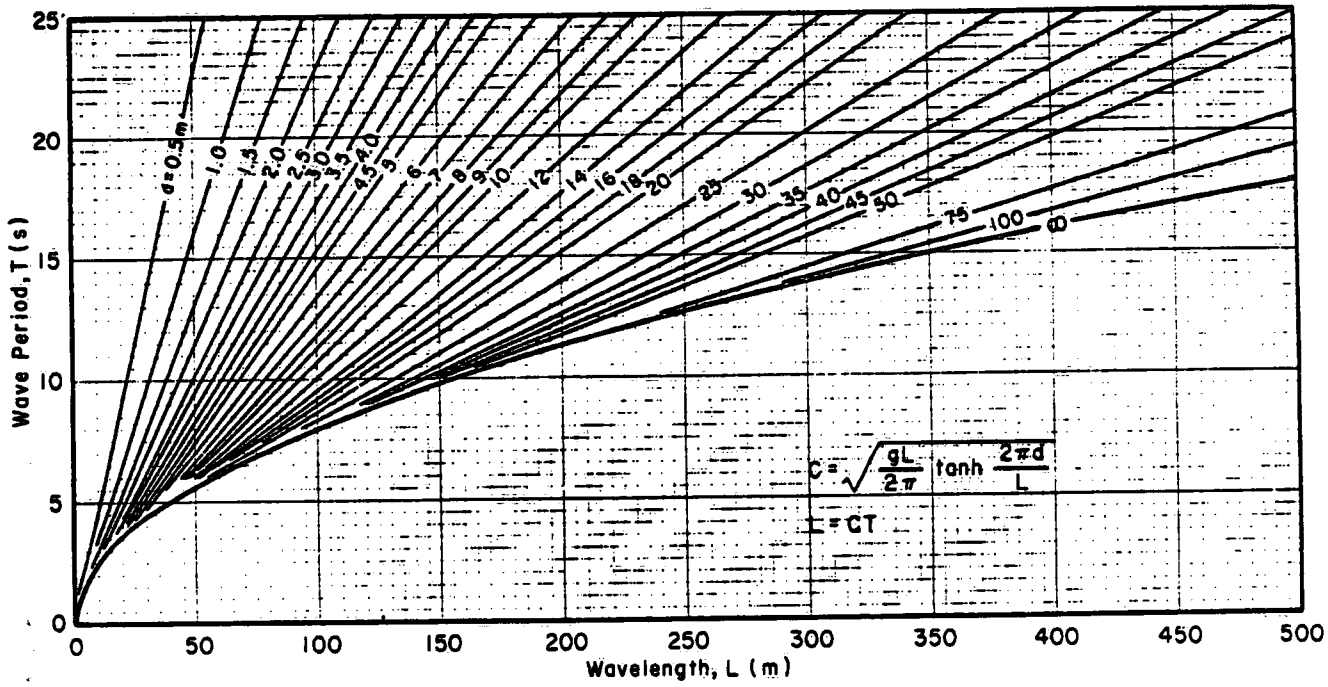

Figure 4. Relationship between wavelength, wave period and depth (Shore Protection Manual 1984).

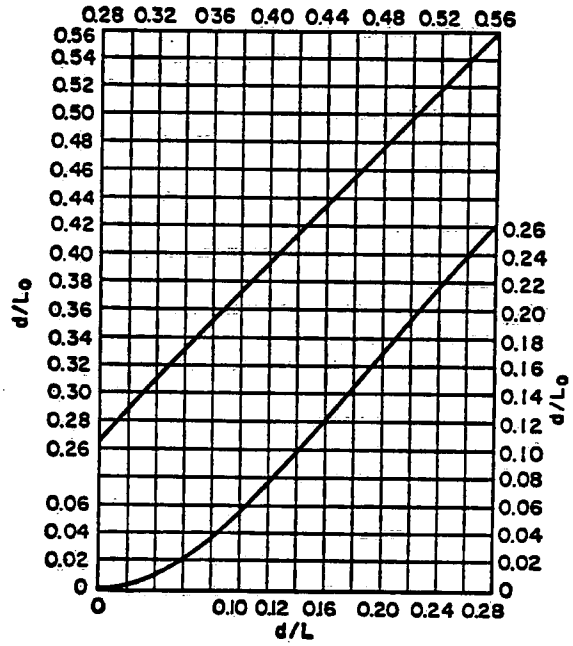

Figure 5. d/L versus d/L_0 (Brater and King 1976).

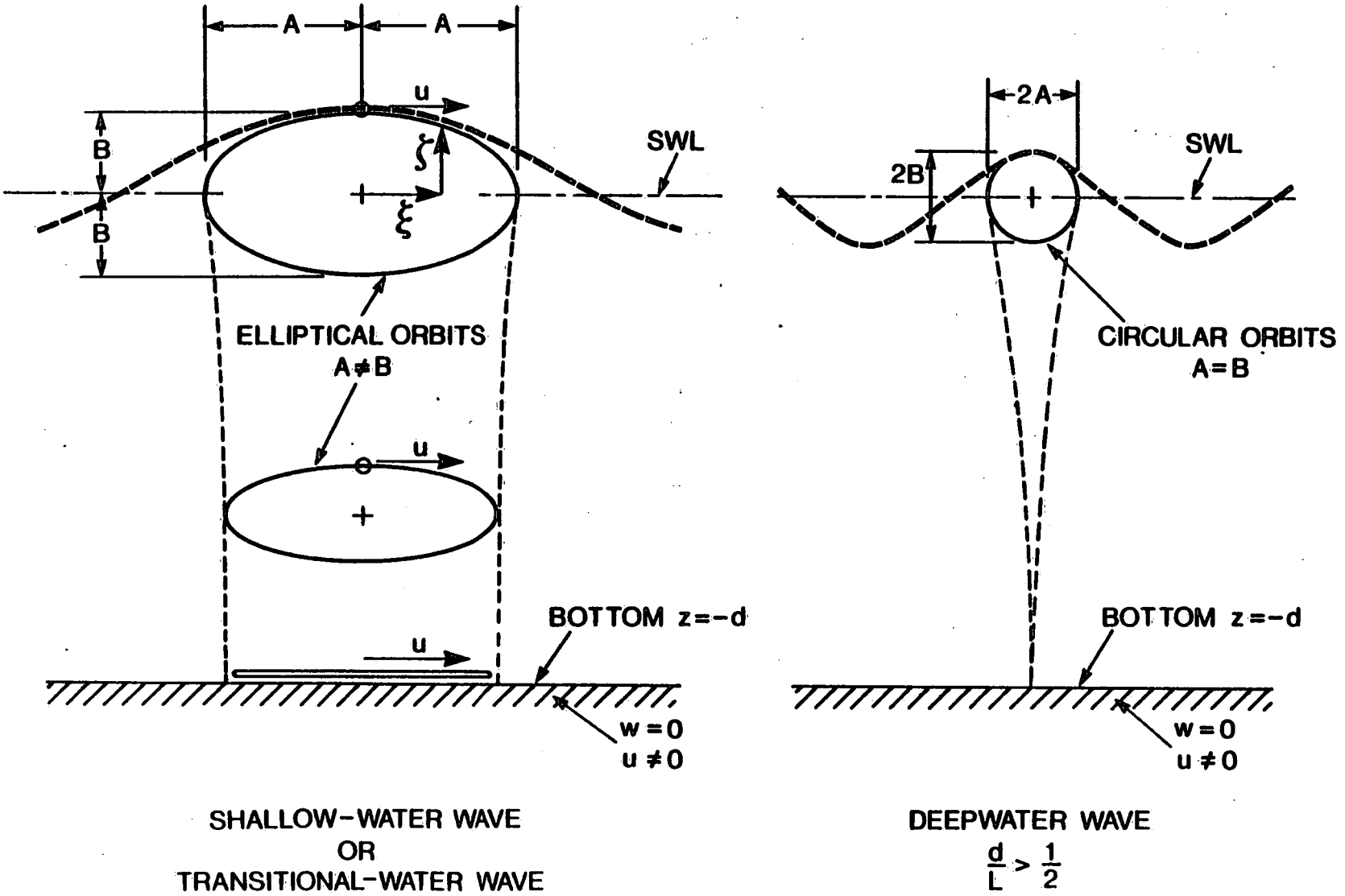

Figure 6. Representation of water particle motions (Shore Protection Manual 1984).

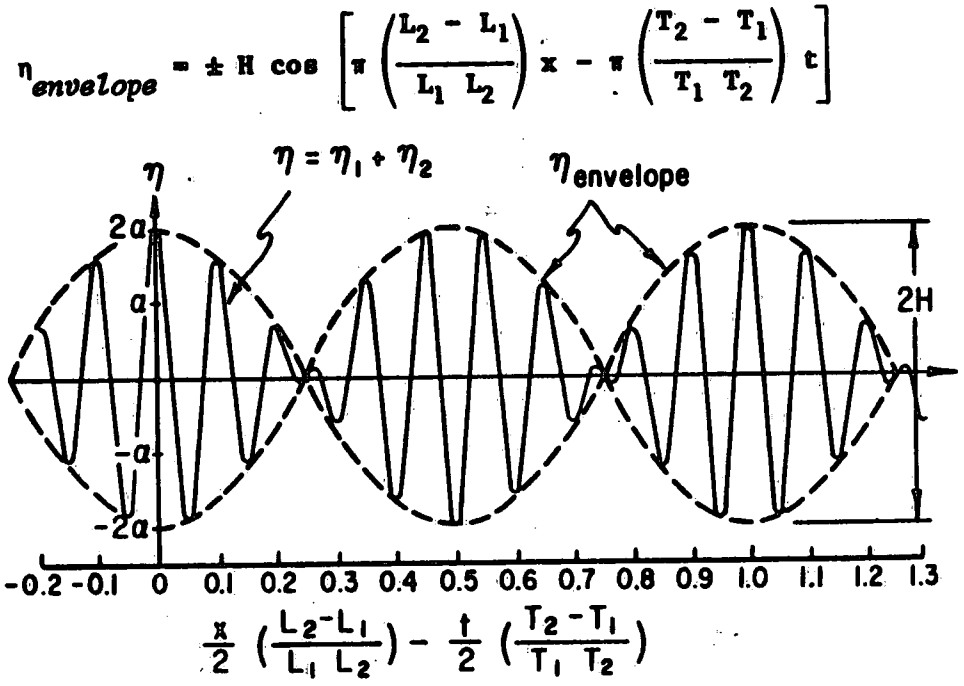

Figure 7. Formation of wave groups by the additon of two sinusoids having different periods (after Kinsman 1965, Shore Protection Manual 1984).

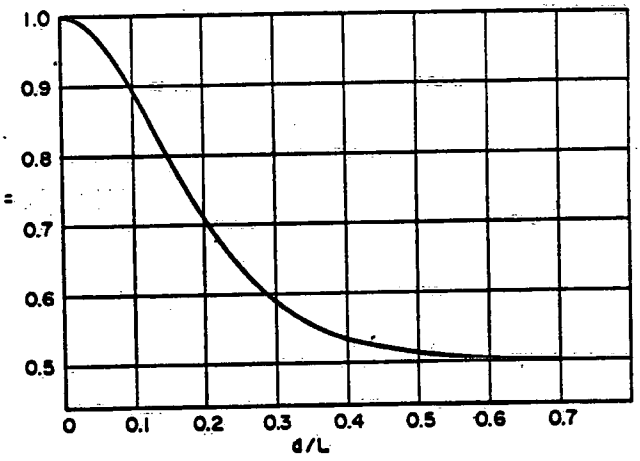

Figure 8. The group velocity to phase velocity ratio n versus d/L (Brater and King 1976).

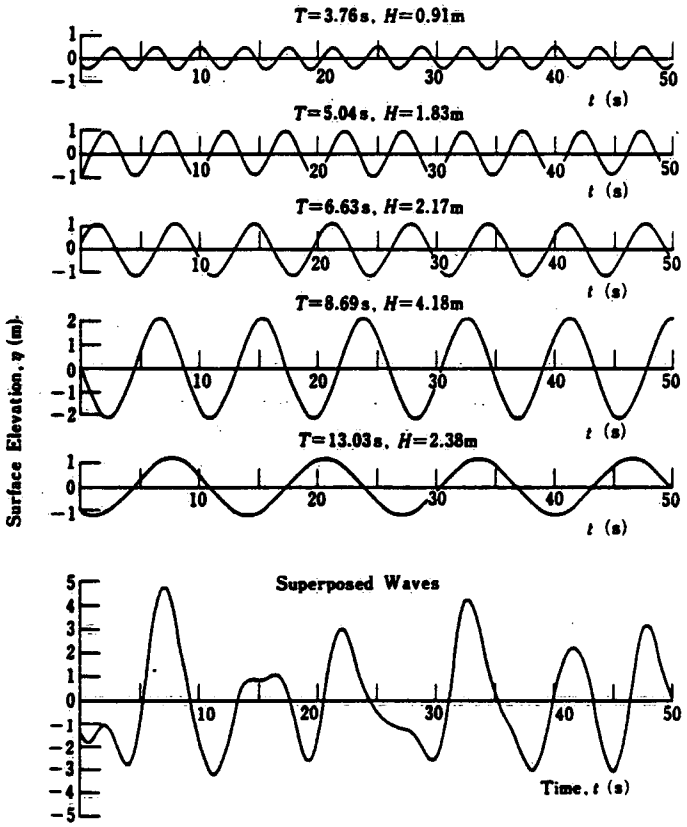

Figure 9. Simulation of irregular waves by superposition of five trains of sinusoidal waves (Goda 1985).

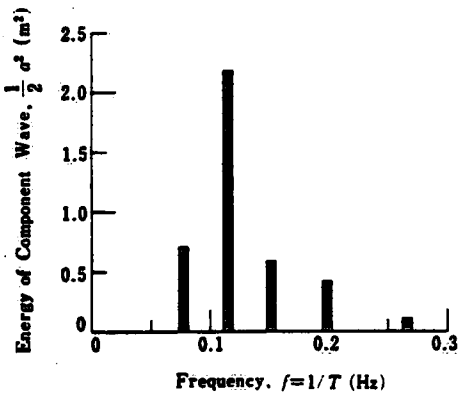

Figure 10. Spectral representation of waves of Figure 9 (Goda 1985).

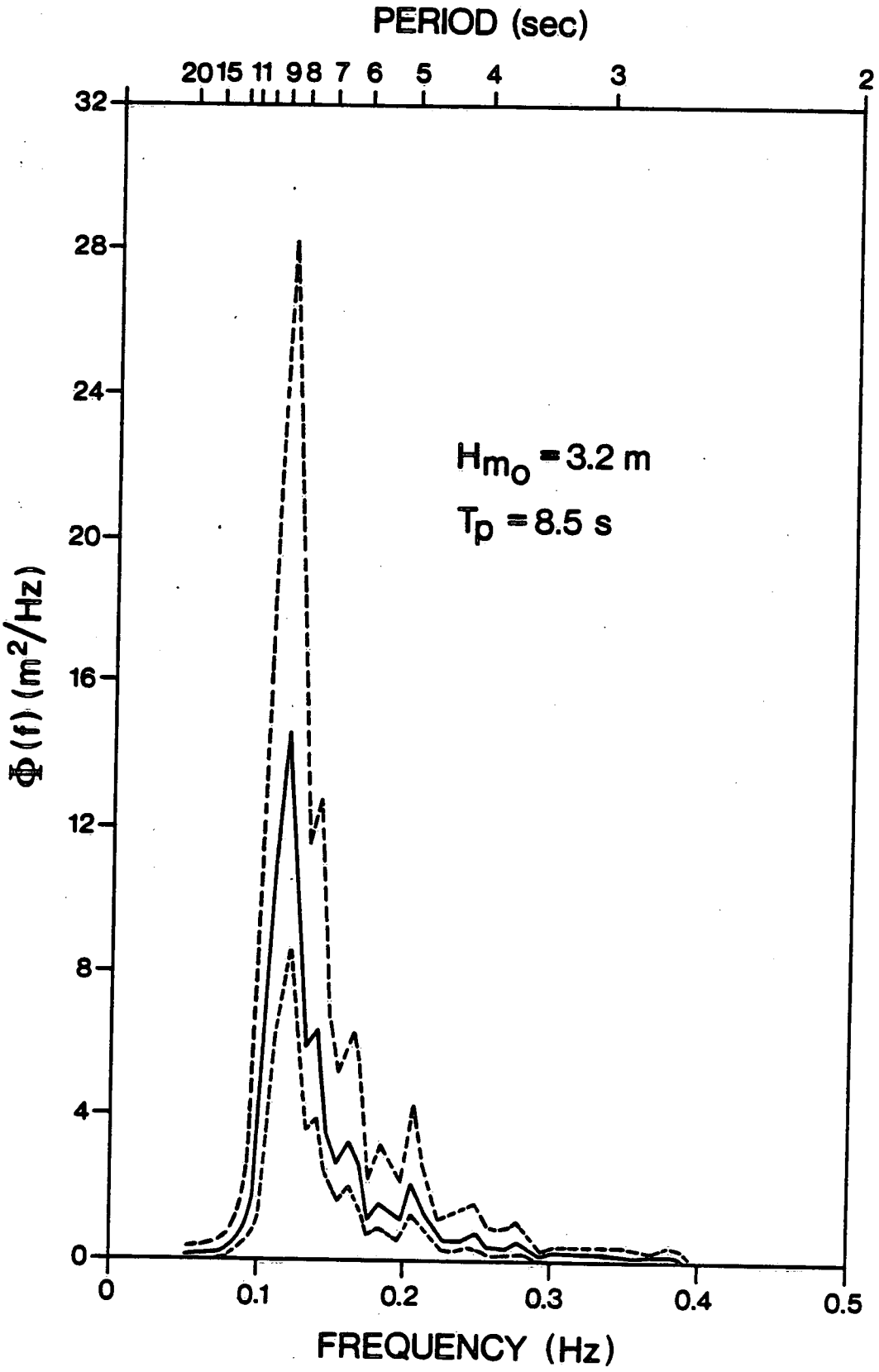

Figure 11. Spectrum measured by an accelerometer buoy (ARSLOE Station 910) off Duck, North Carolina, October, 1980 (dashed curves indicate 90% confidence limits).

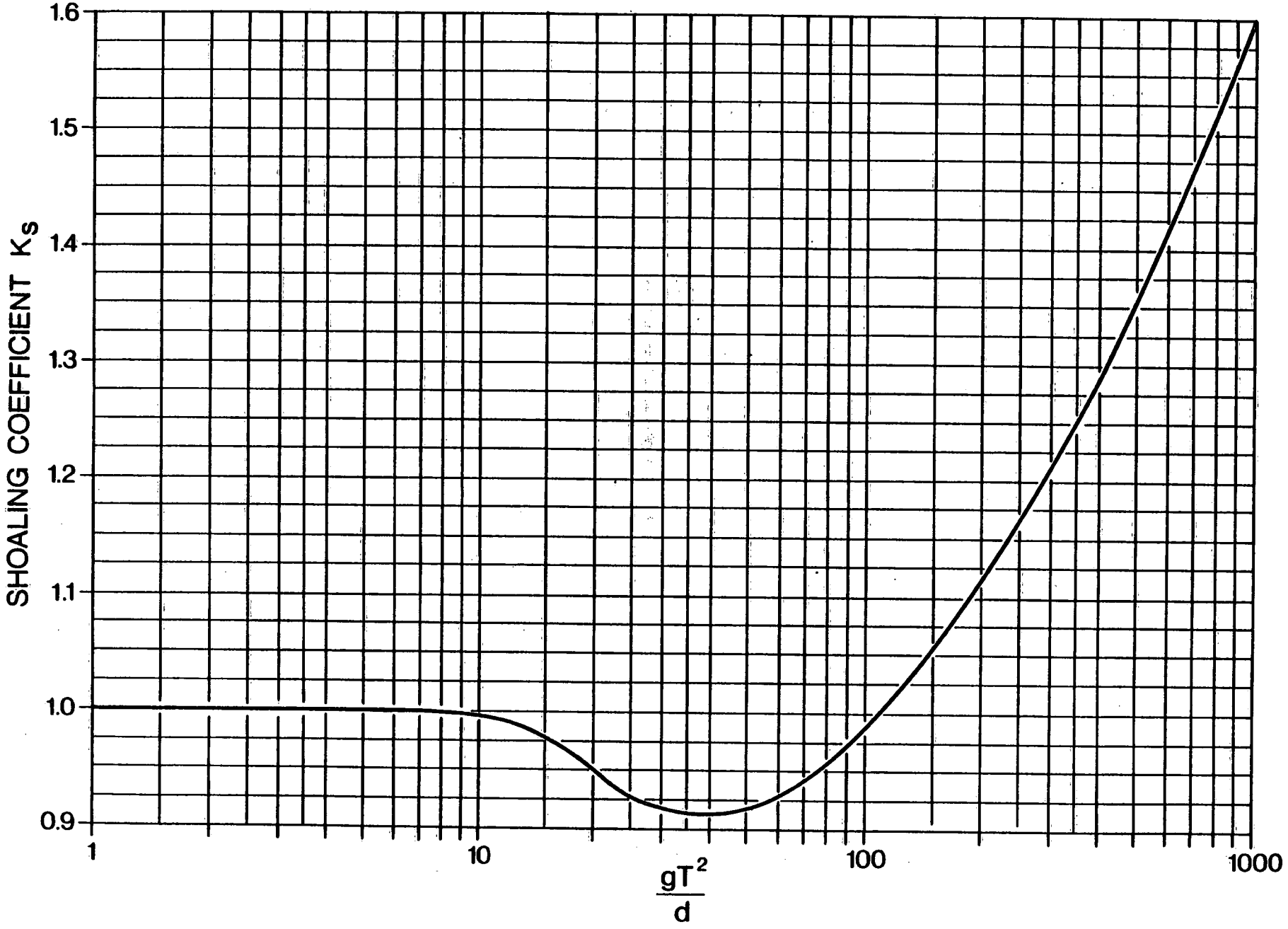

Figure 12. Shoaling coefficient versus gT^2/d.

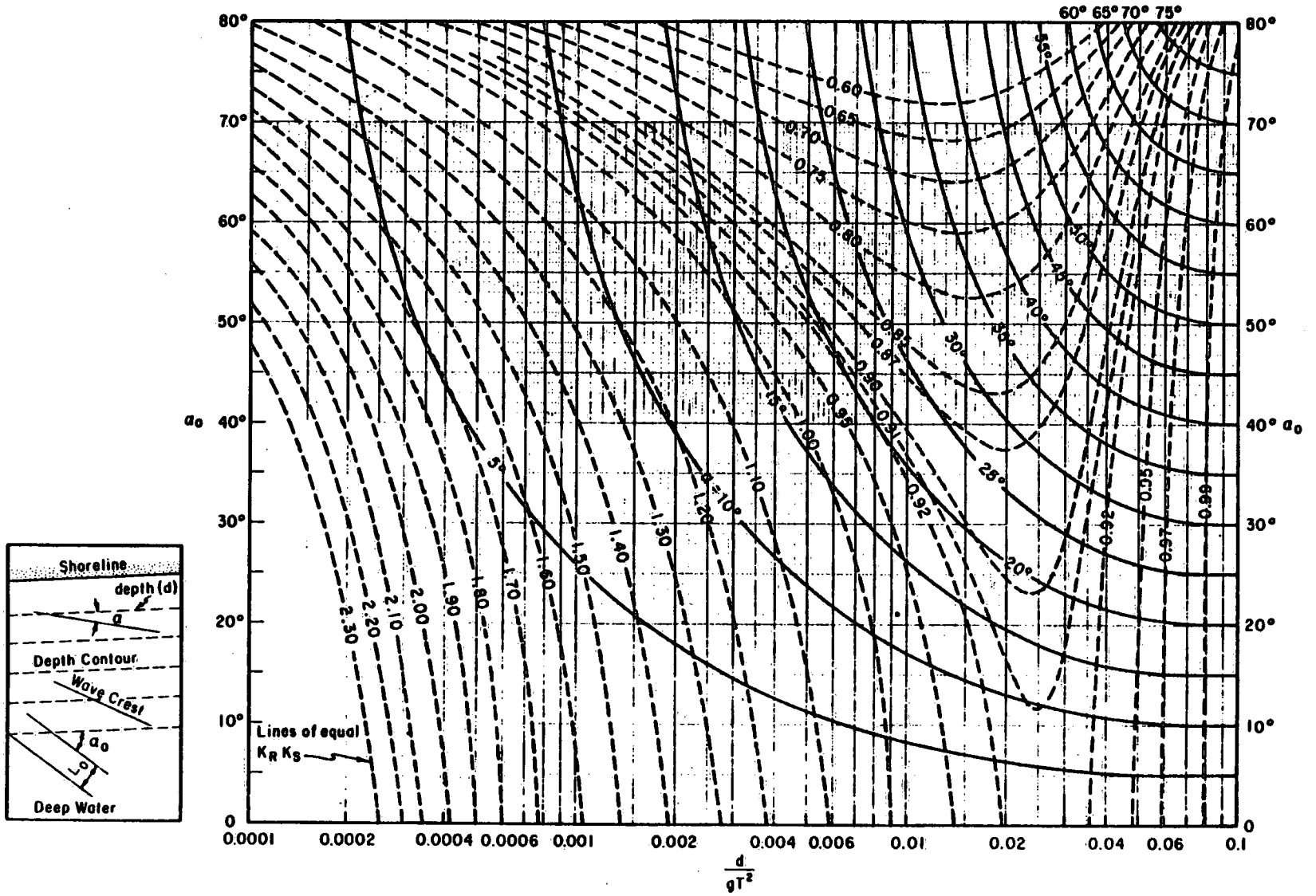

Figure 13. Change in wave direction and height due to refraction and shoaling on slopes with straight, parallel depth contours (Shore Protection Manual 1984).

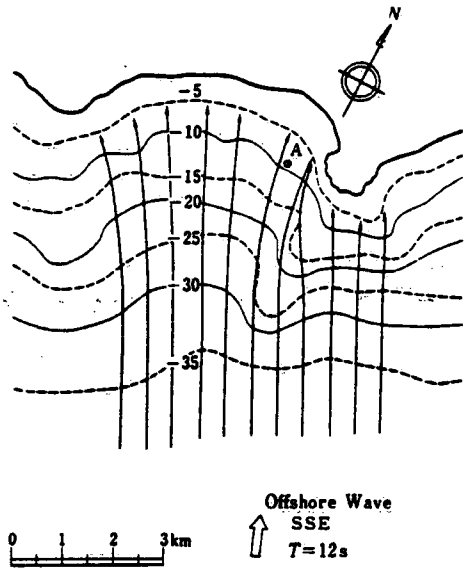

Figure 14. Example of wave refraction diagram (Goda 1985).

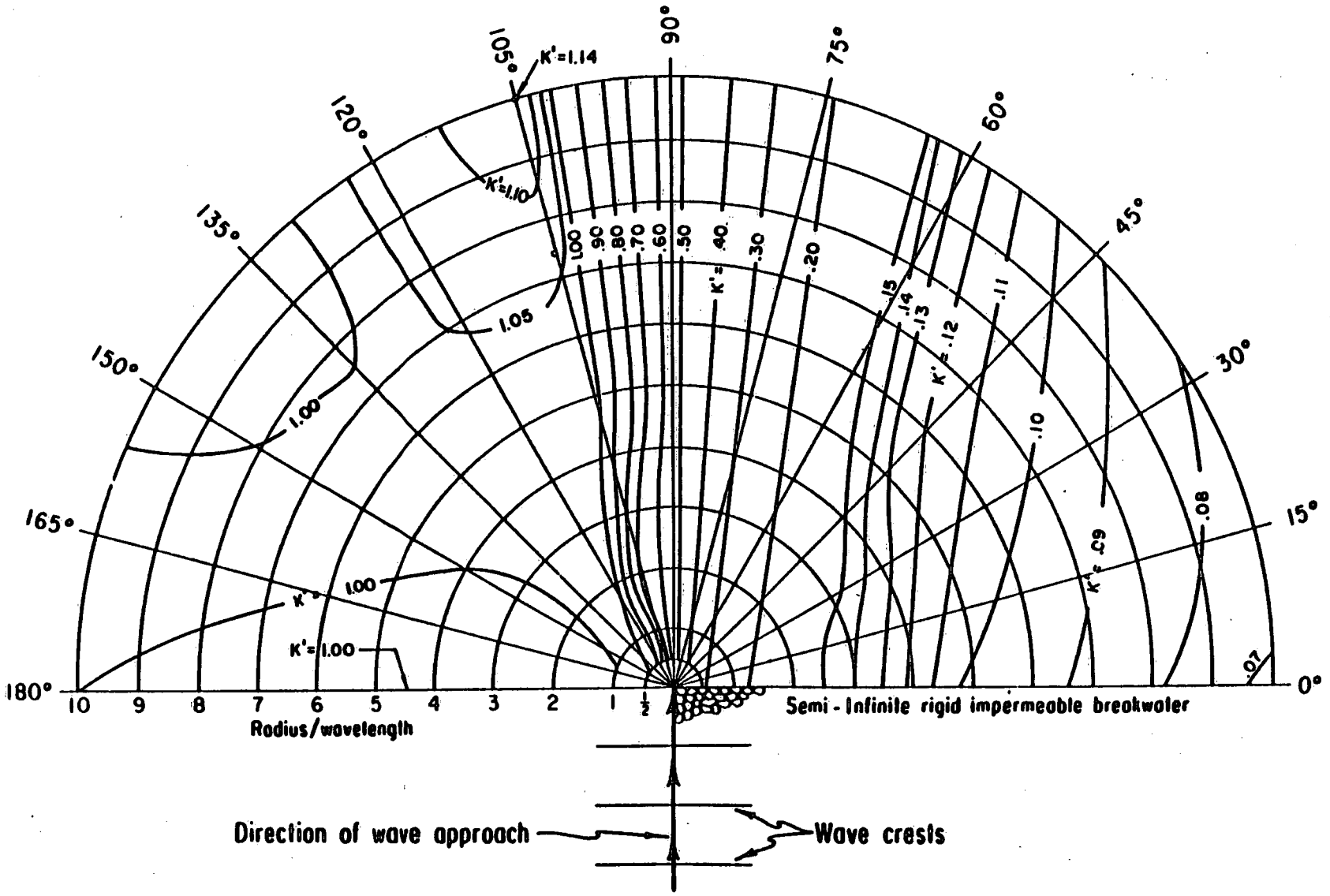

Figure 15. Wave diffraction diagram for monochromatic waves approaching normal to a semi-infinite rigid impermeable breakwater (after Wiegel 1962, Shore Protection Manual 1984).

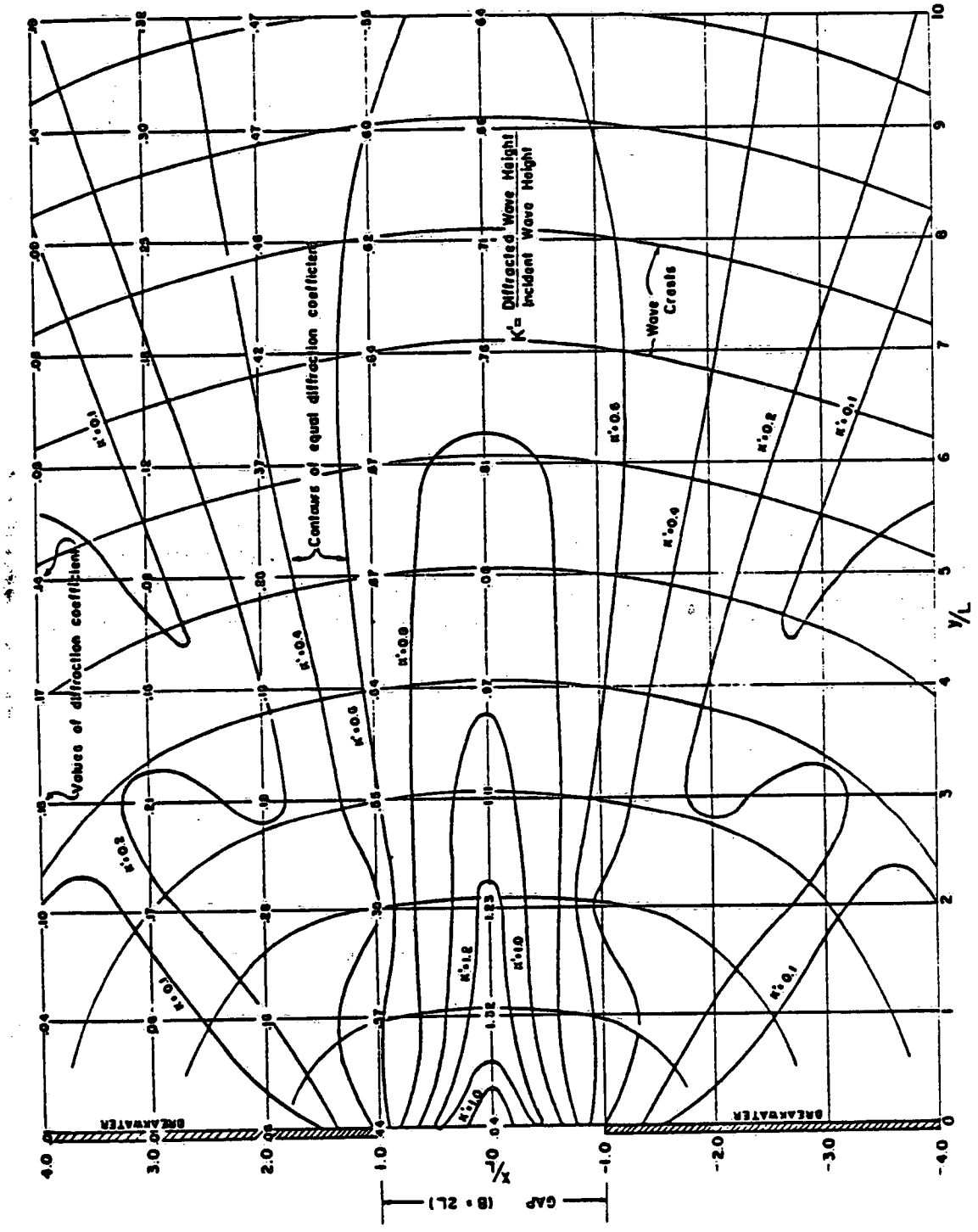

Figure 16. Wave diffraction diagram for monochromatic waves approaching normal to a breakwater gap of two wavelengths (Shore Protection Manual 1984).

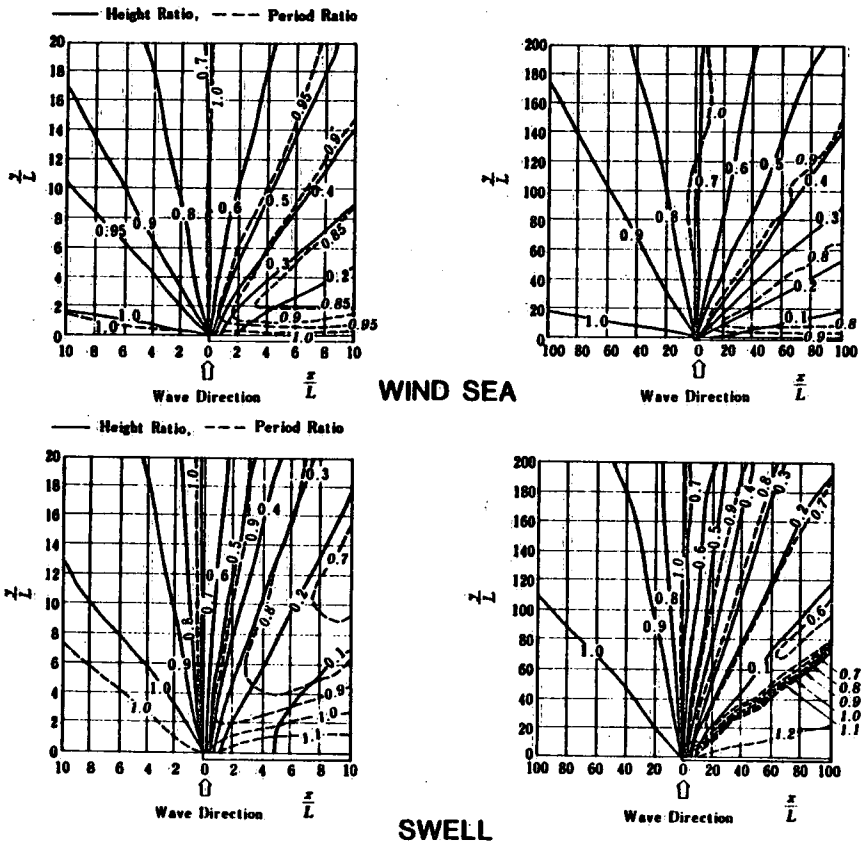

Figure 17. Wave diffraction diagram for irregular waves approaching normal to a semi-infinite rigid impermeable breakwater (solid lines for wave height ratio and dashed lines for wave period ratio) (Goda 1985).

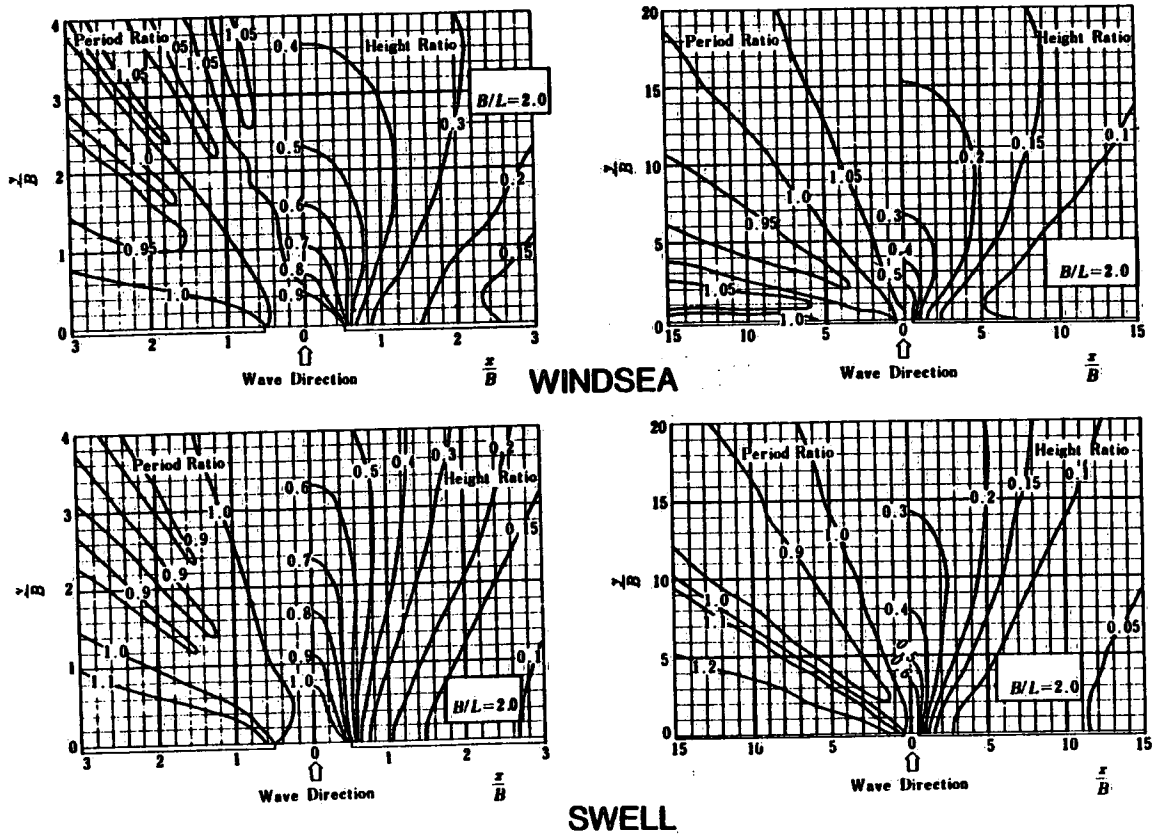

Figure 18. Wave diffraction diagram for irregular waves approaching normal to a breakwater gap (B) of two wavelengths (Goda 1985).

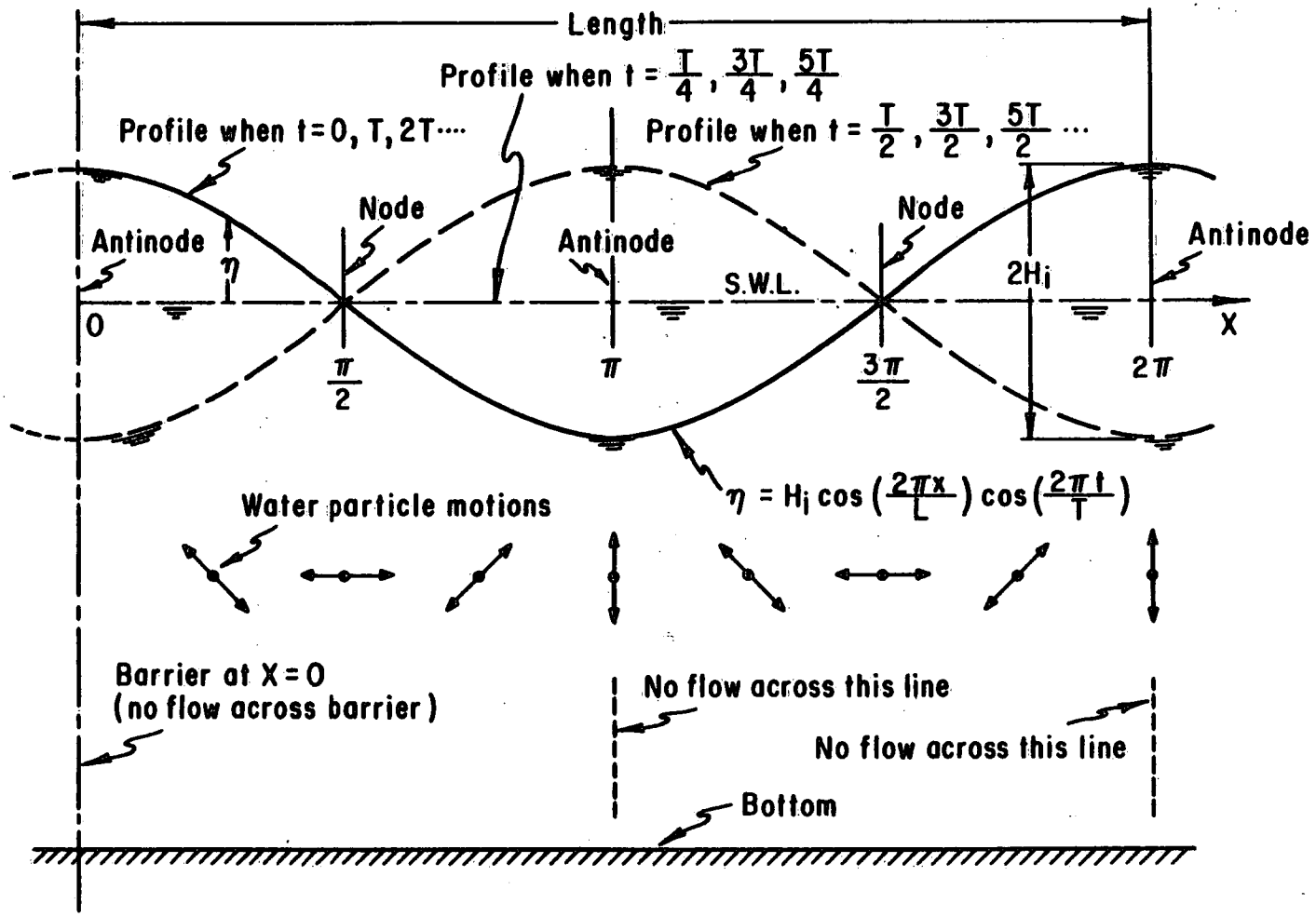

Figure 19. Definition sketch for a standing wave system (Shore Protection Manual 1984).

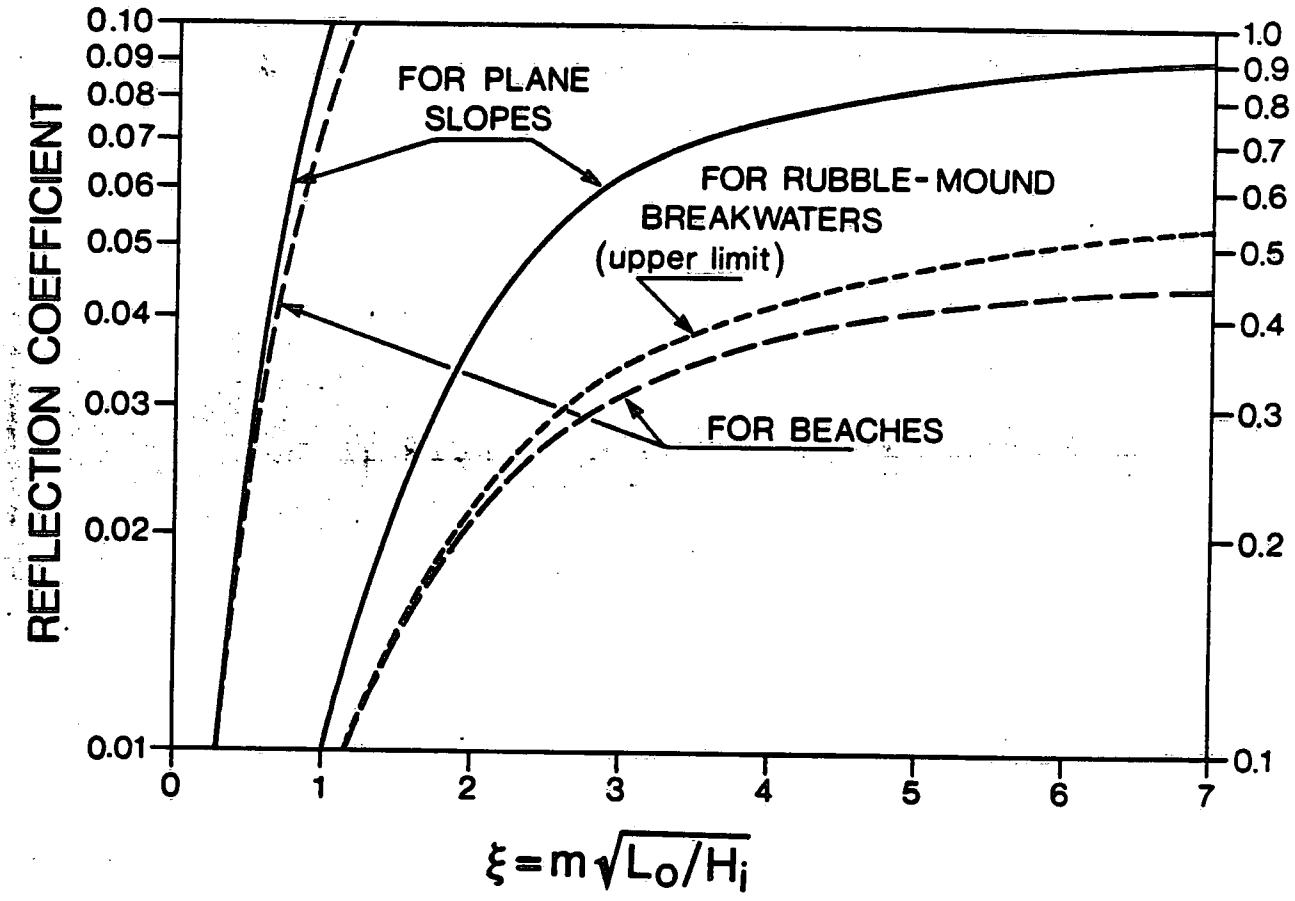

Figure 20. Wave reflection coefficients for slopes, beaches and rubble-mound breakwaters (after Shore Protection Manual 1984).

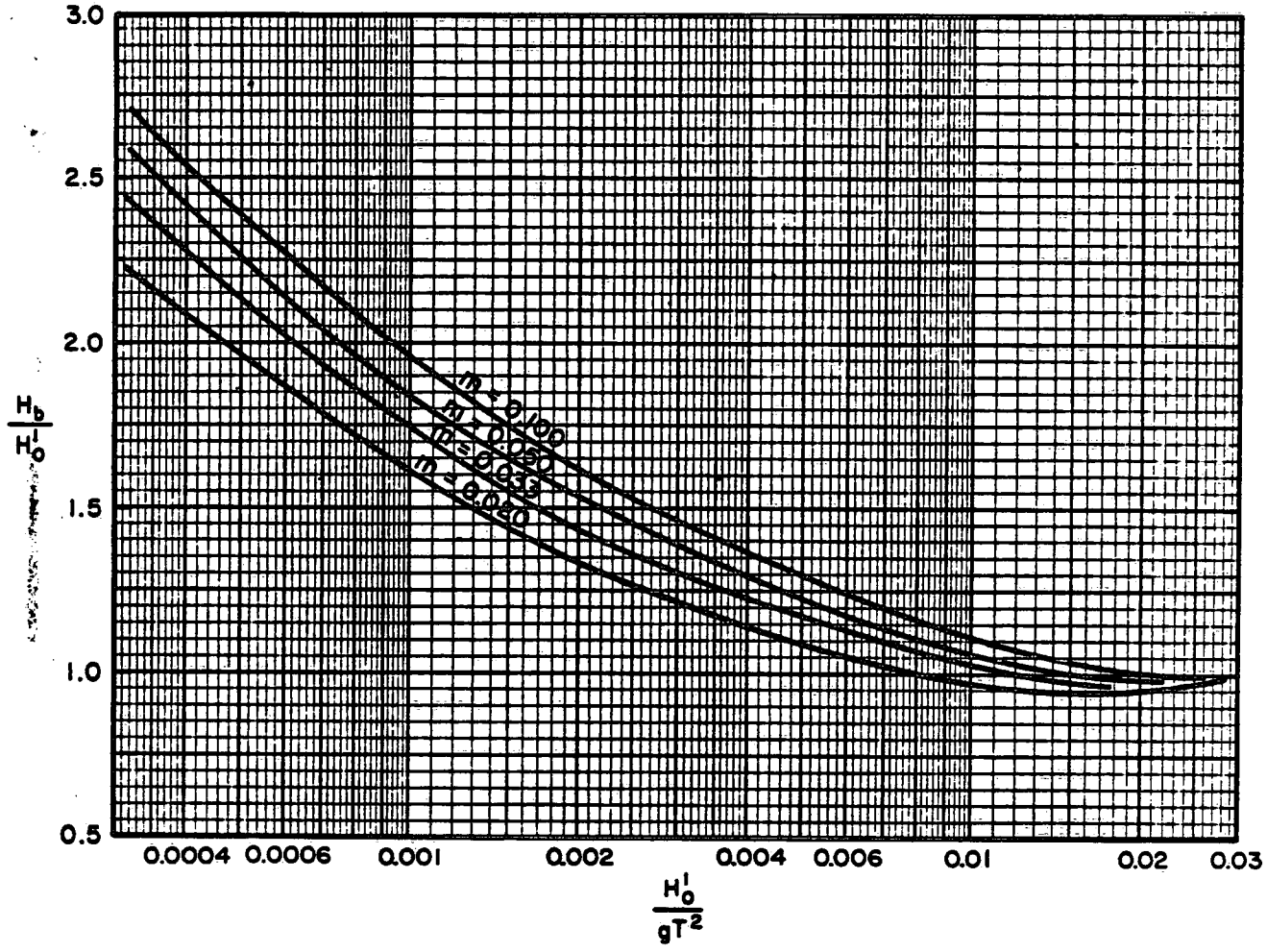

Figure 21. H_b/H_0' versus H_0'/gT^2 with m = beach slope (after Goda 1970, Shore Protection Manual 1984).

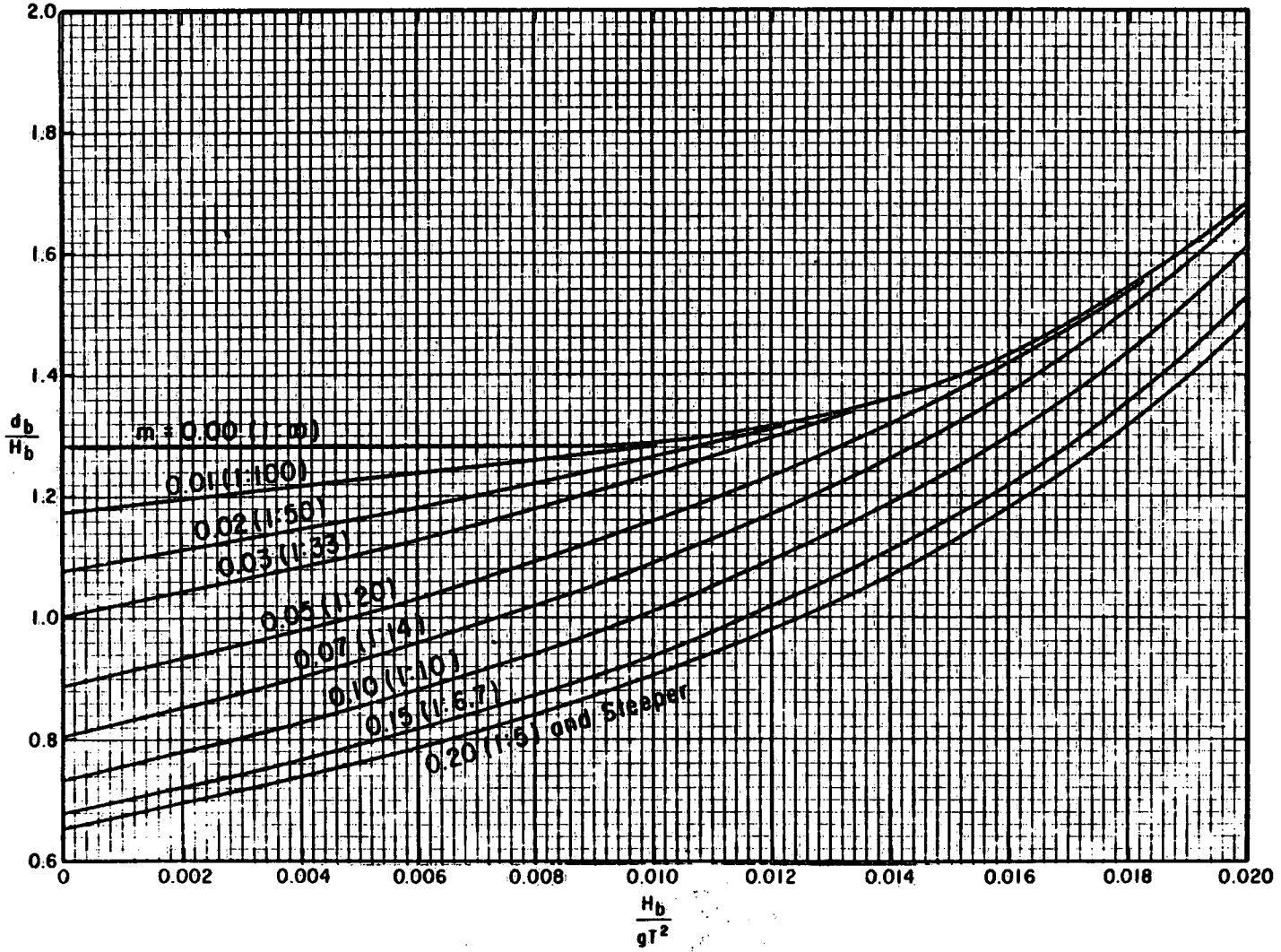

Figure 22. d_b/H_b versus H_b/gT^2 with m = beach slope (Shore Protection Manual 1984).

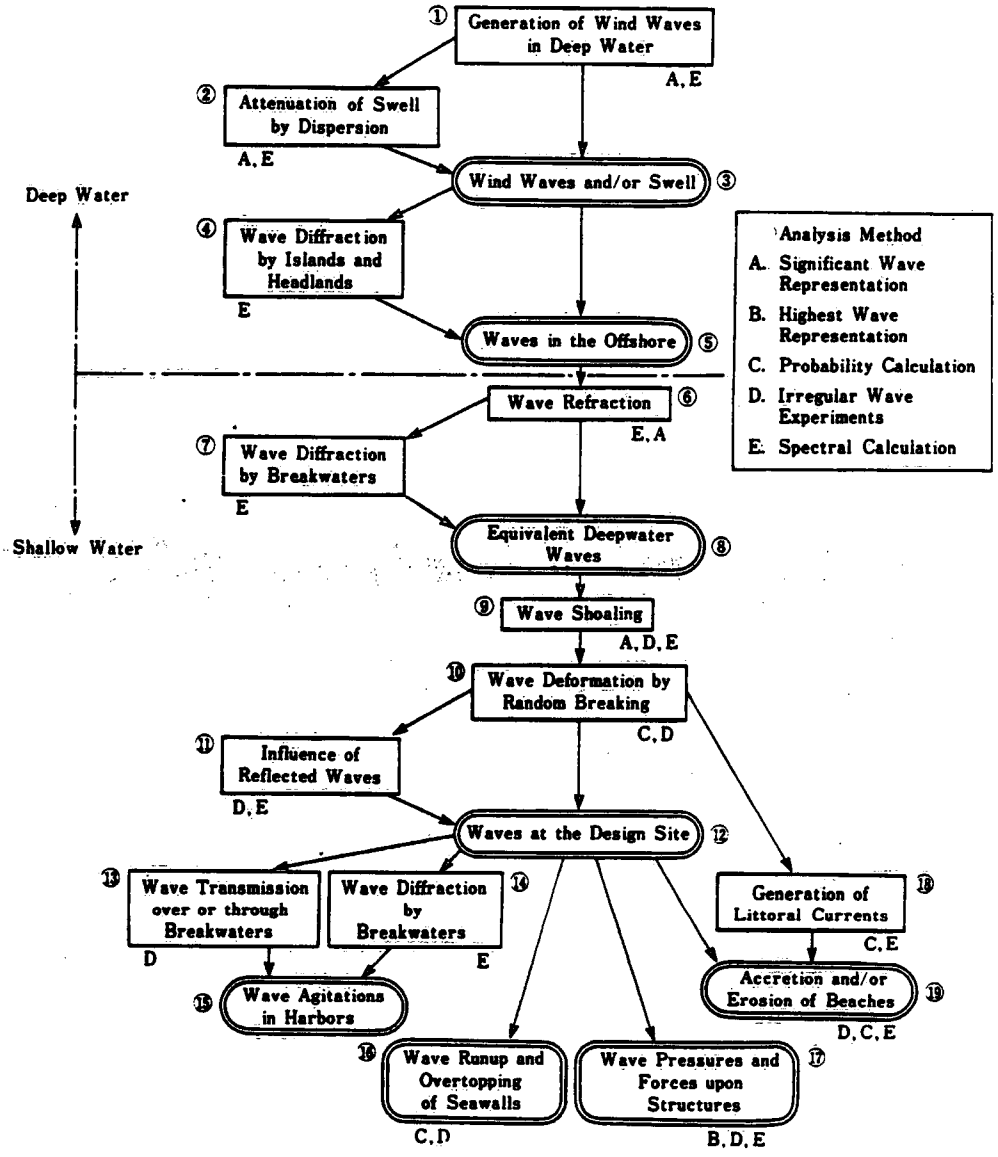

Figure 23. Flow of the transformations and actions of sea waves with suggested methods for their calculation (Goda 1985).

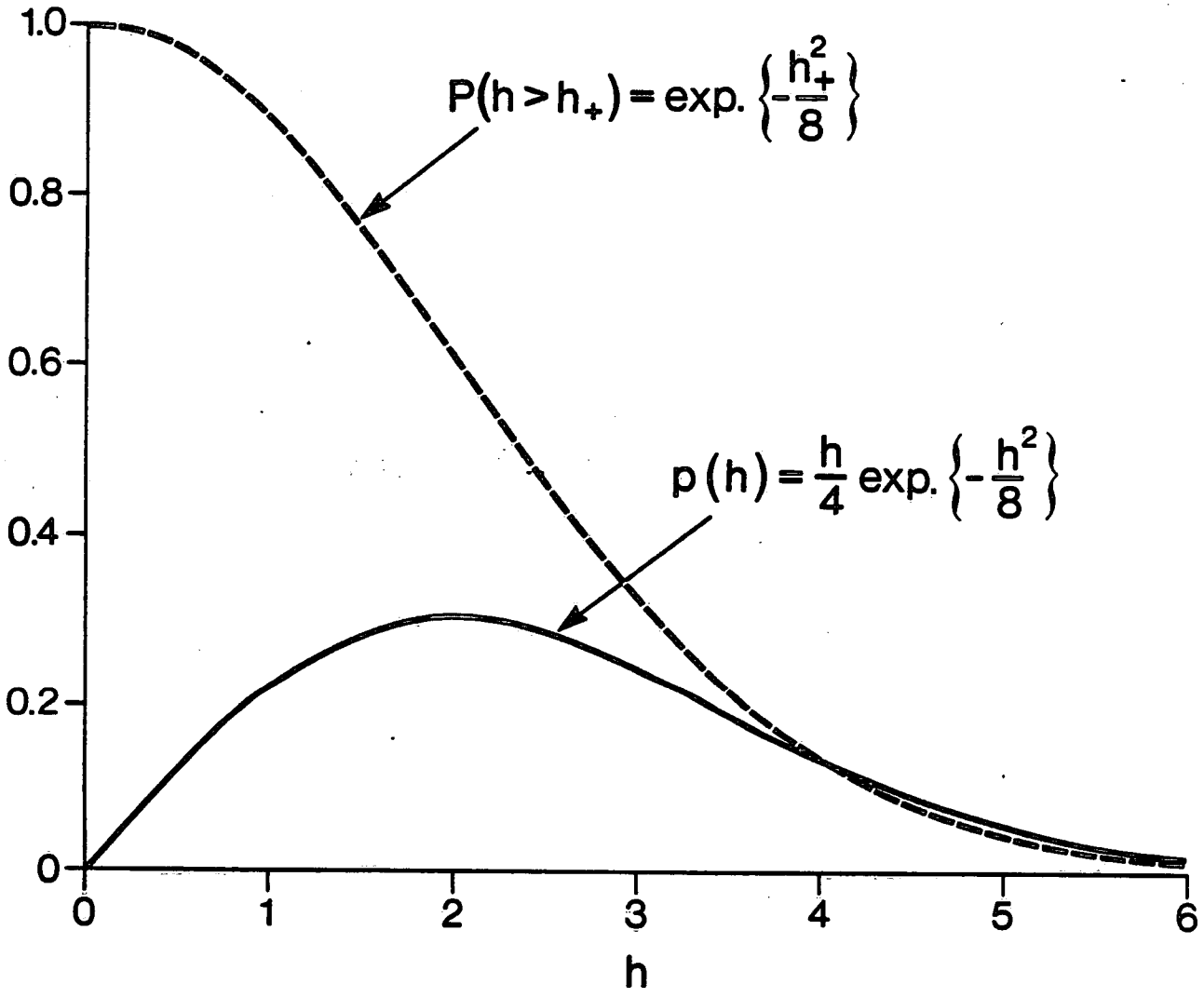

Figure 24. The probability distribution of normalized wave heights p(h) (Rayleigh) and the cumulative distribution, P(h).

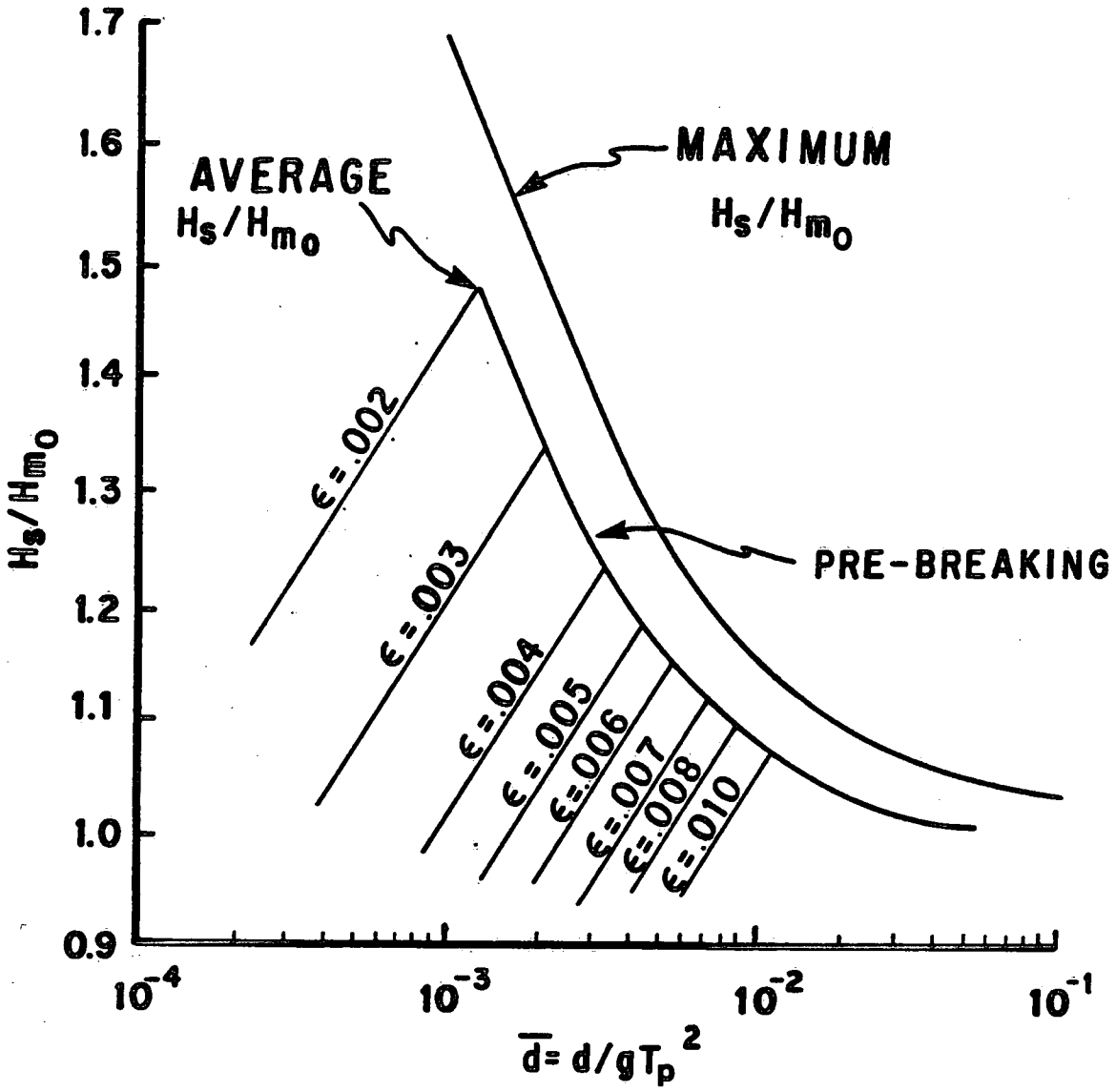

Figure 27. Relation between H_s and H_{m_0} in shoaling water (after Thompson and Vincent 1985).

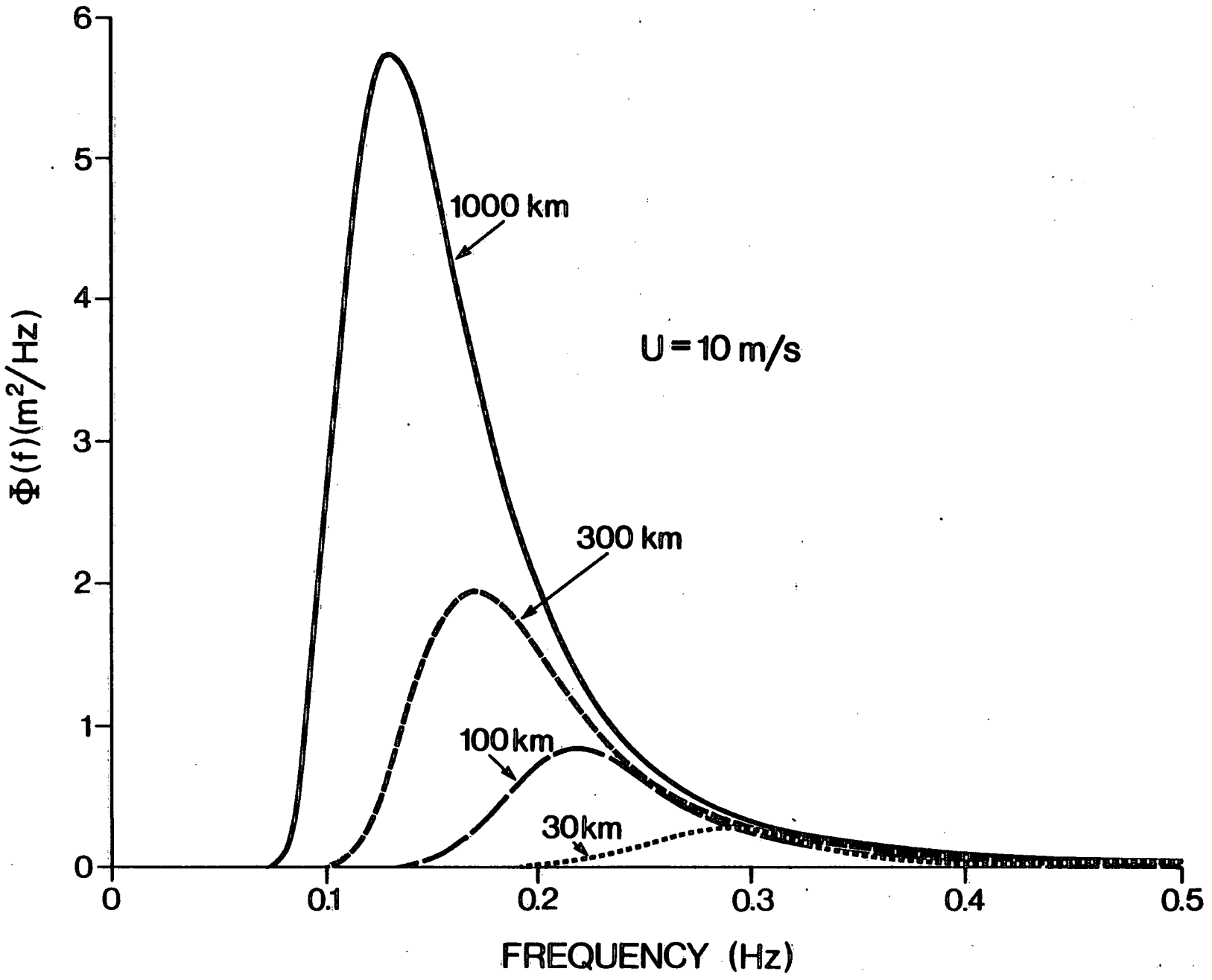

Figure 28. Spectra from Equation 64 for a 10 m/s wind (at 10 m height) and various fetches.

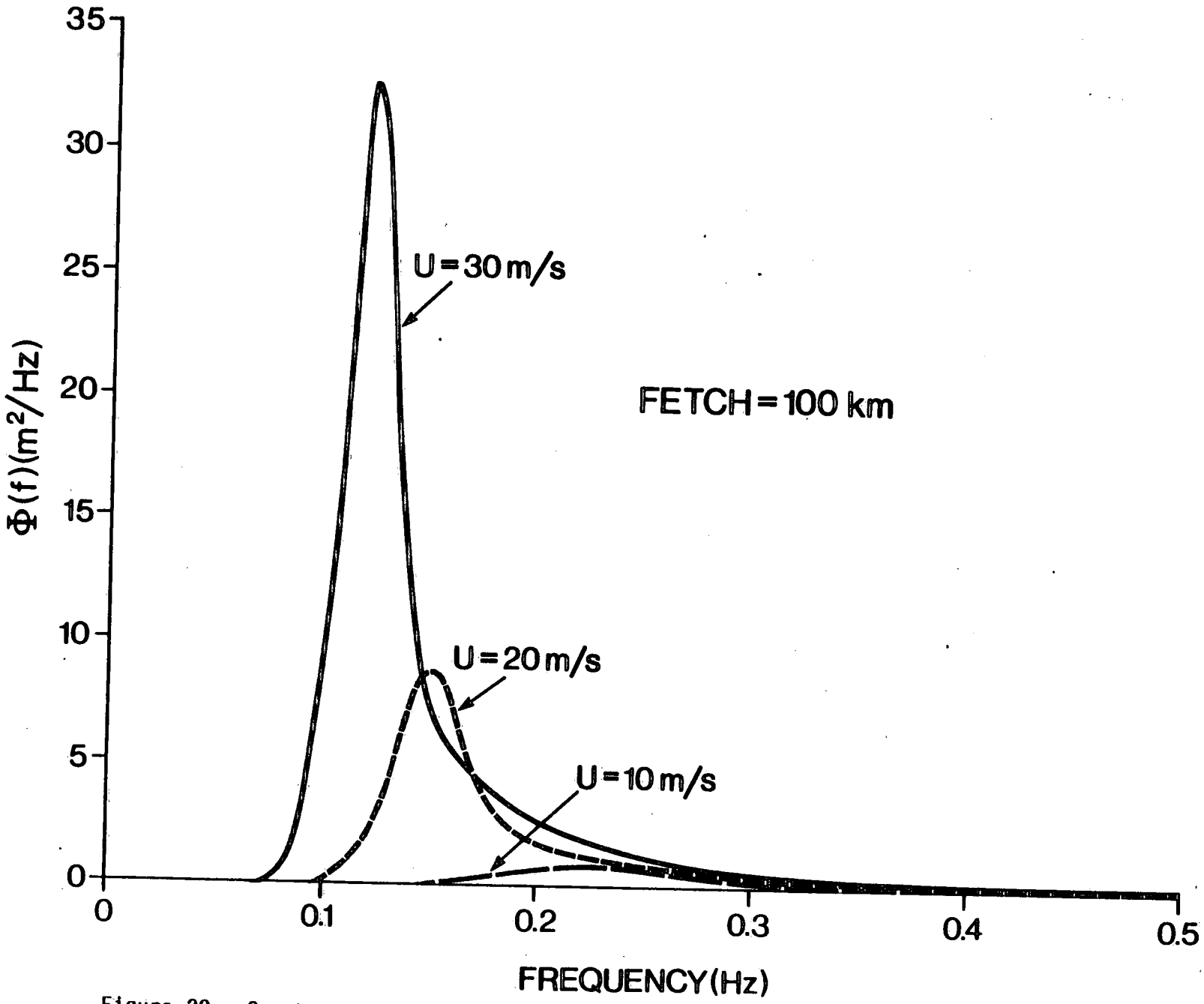

Figure 29. Spectra from Equation 64 at 100 km fetch and various wind speeds.

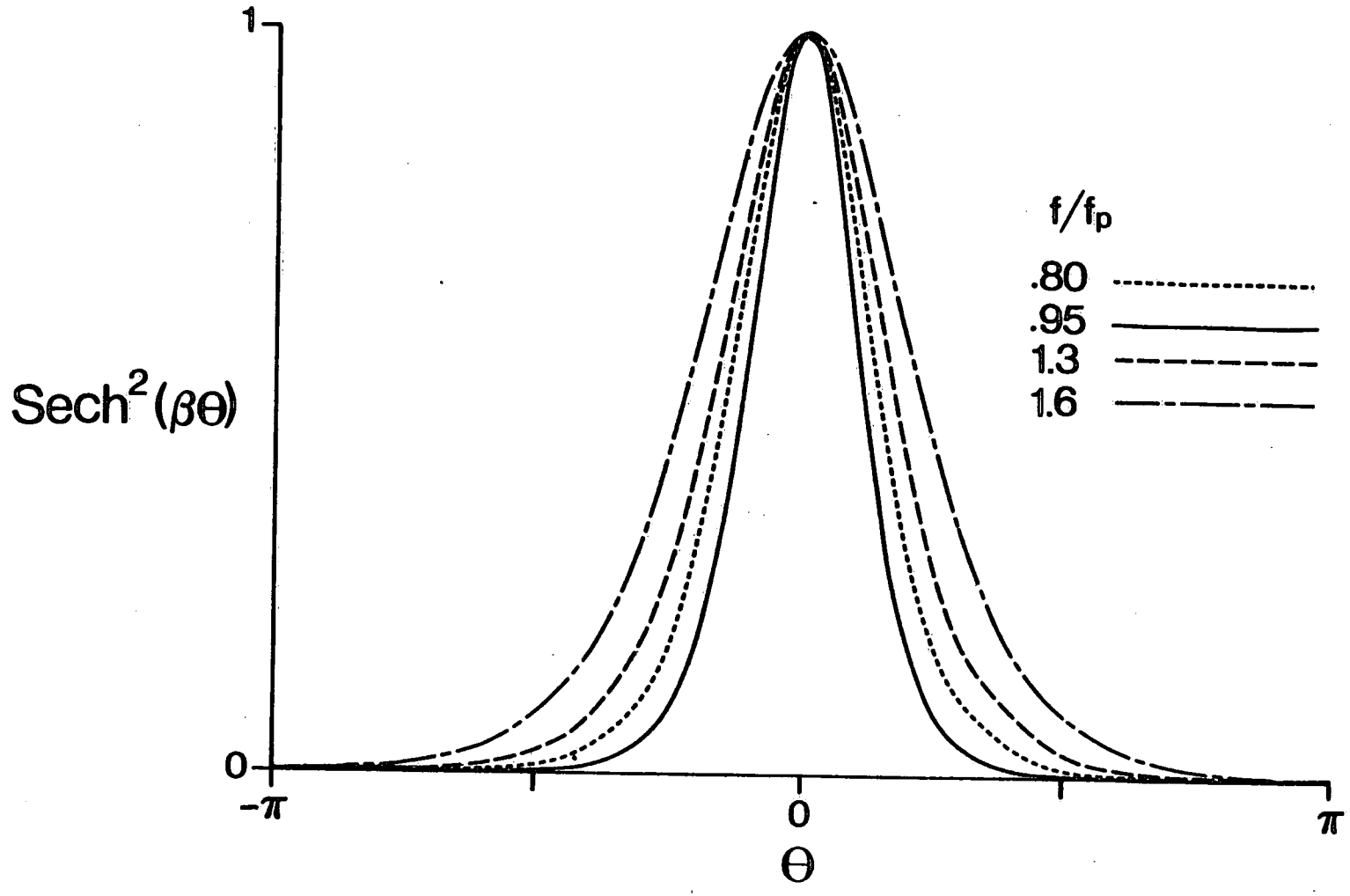

Figure 30. The directional spreading of wind waves for various frequencies relative to the peak frequency f_p (Donelan et al. 1985).

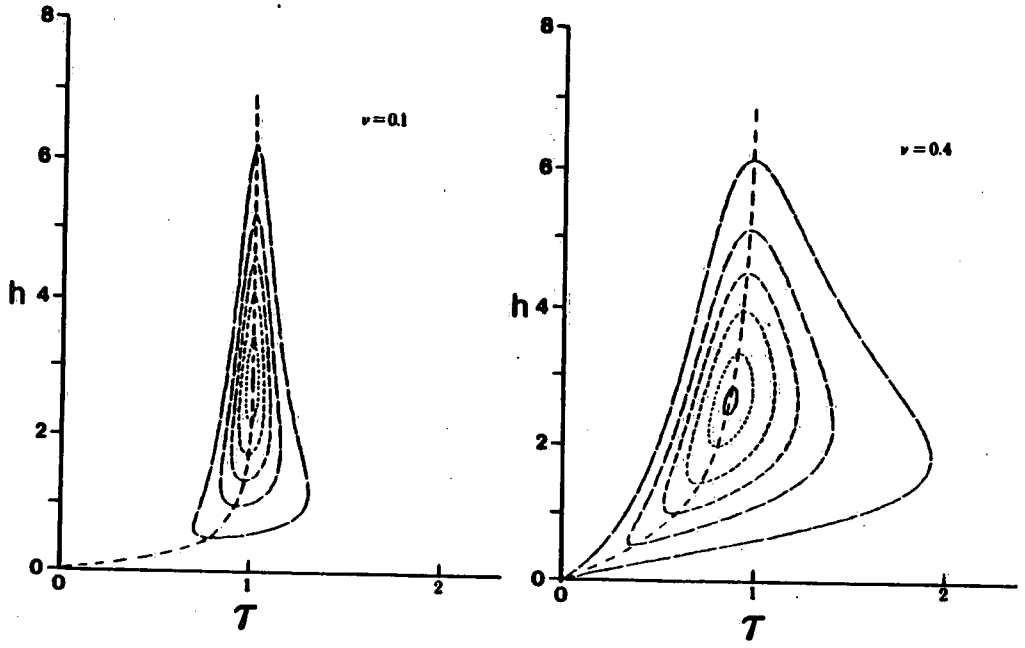

Figure 25. The theoretical joint distribution of normalized heights and periods $p(h,\tau)$ for two values of spectral width: $\nu = 0.1$ is appropriate for swell and $\nu = 0.4$ for a typical wind sea. The contours trace $p/p_{max} = 0.99, 0.90, 0.70, 0.50, 0.30, 0.10$ from the centre contour outwards (after Longuet-Higgins 1983).

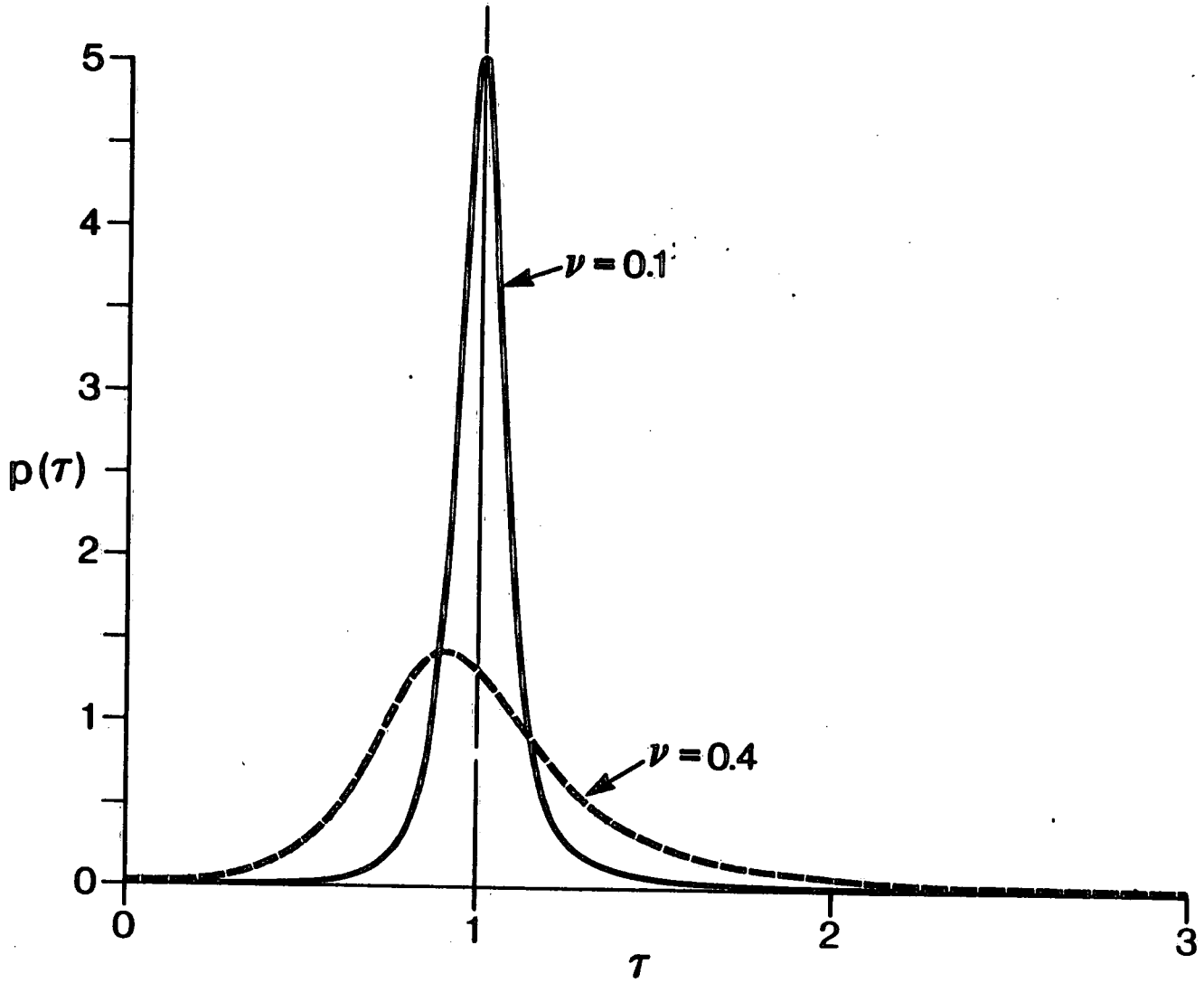

Figure 26. The probability density distribution of normalized periods $p(\tau)$ for values of the spectral width parameter ν = 0.1 and 0.4 (after Longuet-Higgins 1983).

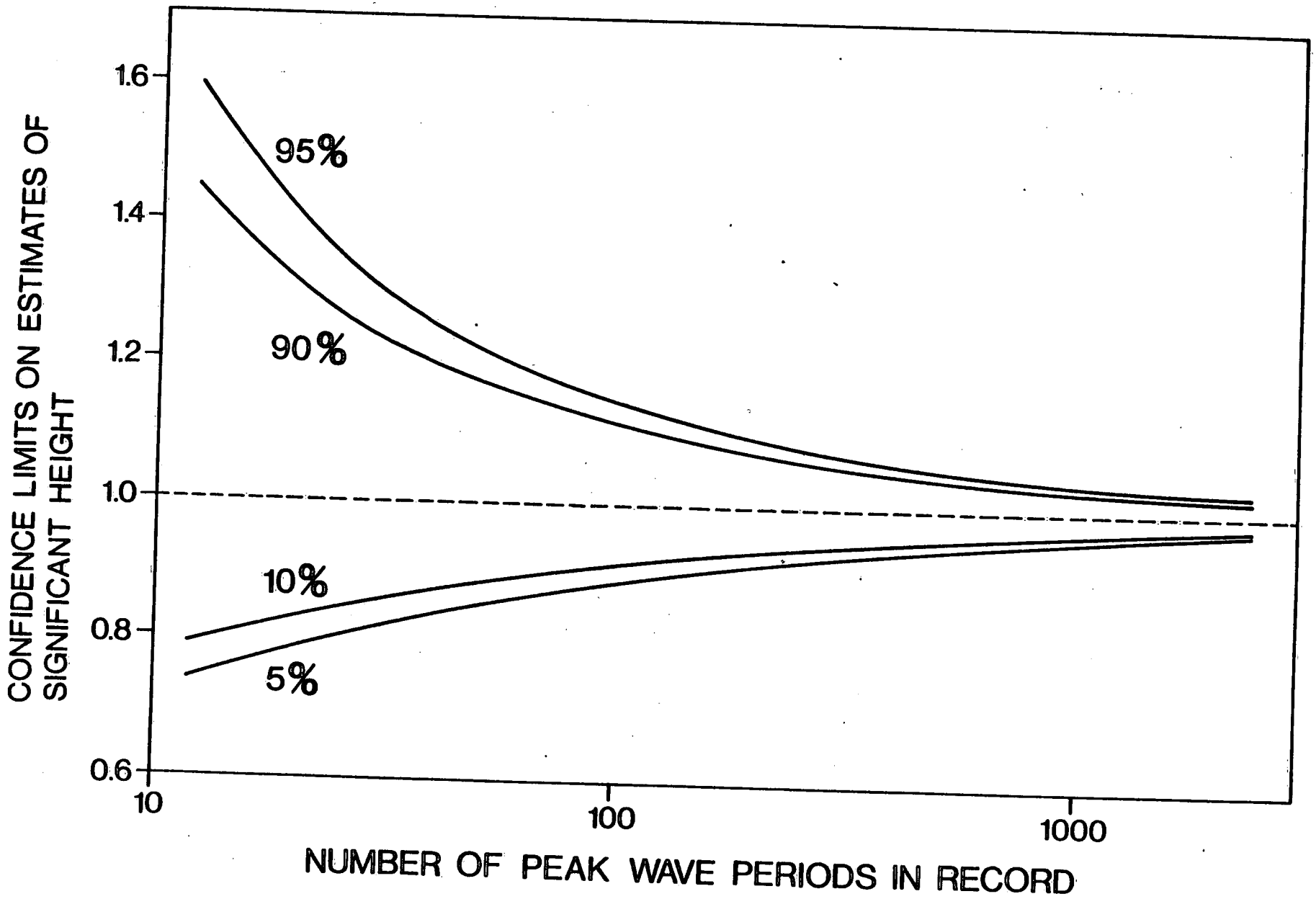

Figure 31. Confidence limits on (relative) significant height as a function of the number of peak wave periods in a record.

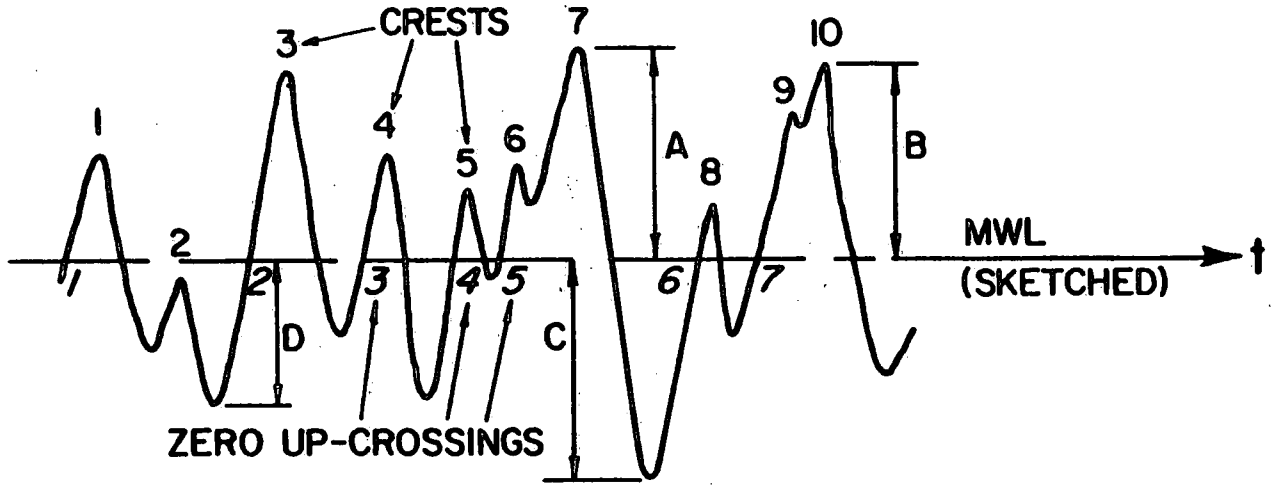

Figure 32. Typical wave record with notation for manual analysis.

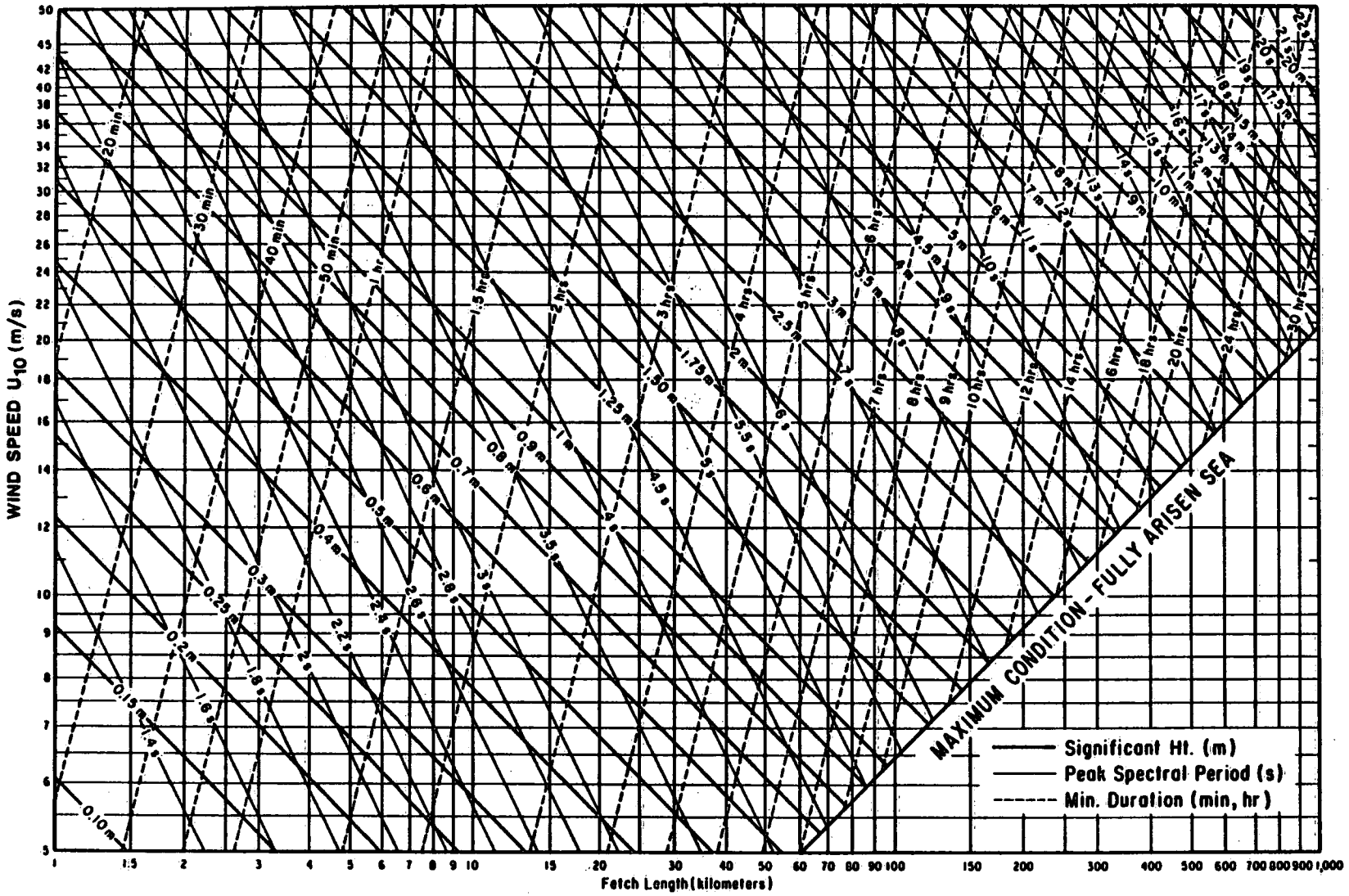

Figure 33. Nomogram of deepwater wave prediction curves (after Shore Protection Manual 1984).

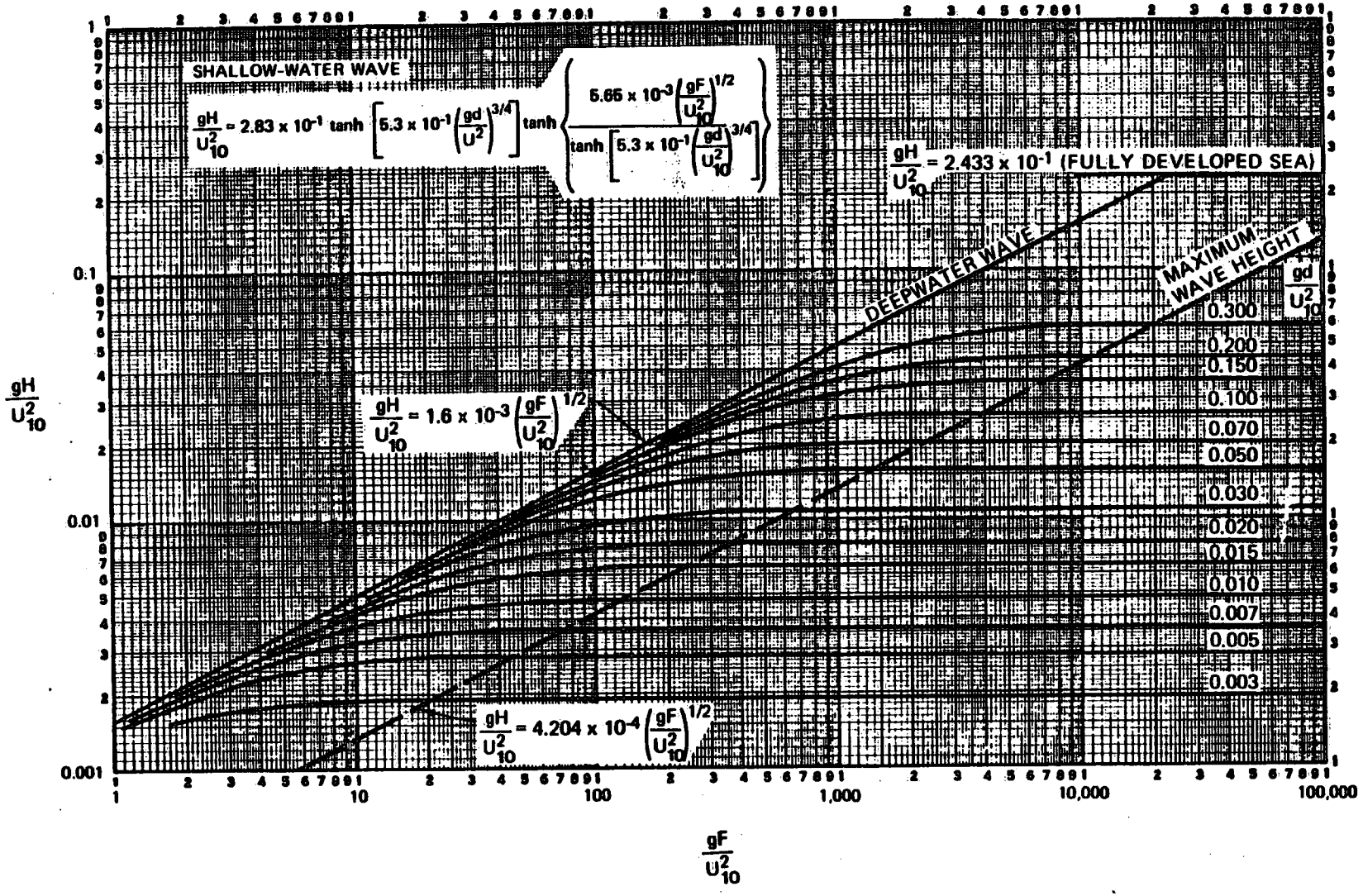

Figure 34. Wave height prediction curves for different values of constant water depth (after Shore Protection Manual 1984).

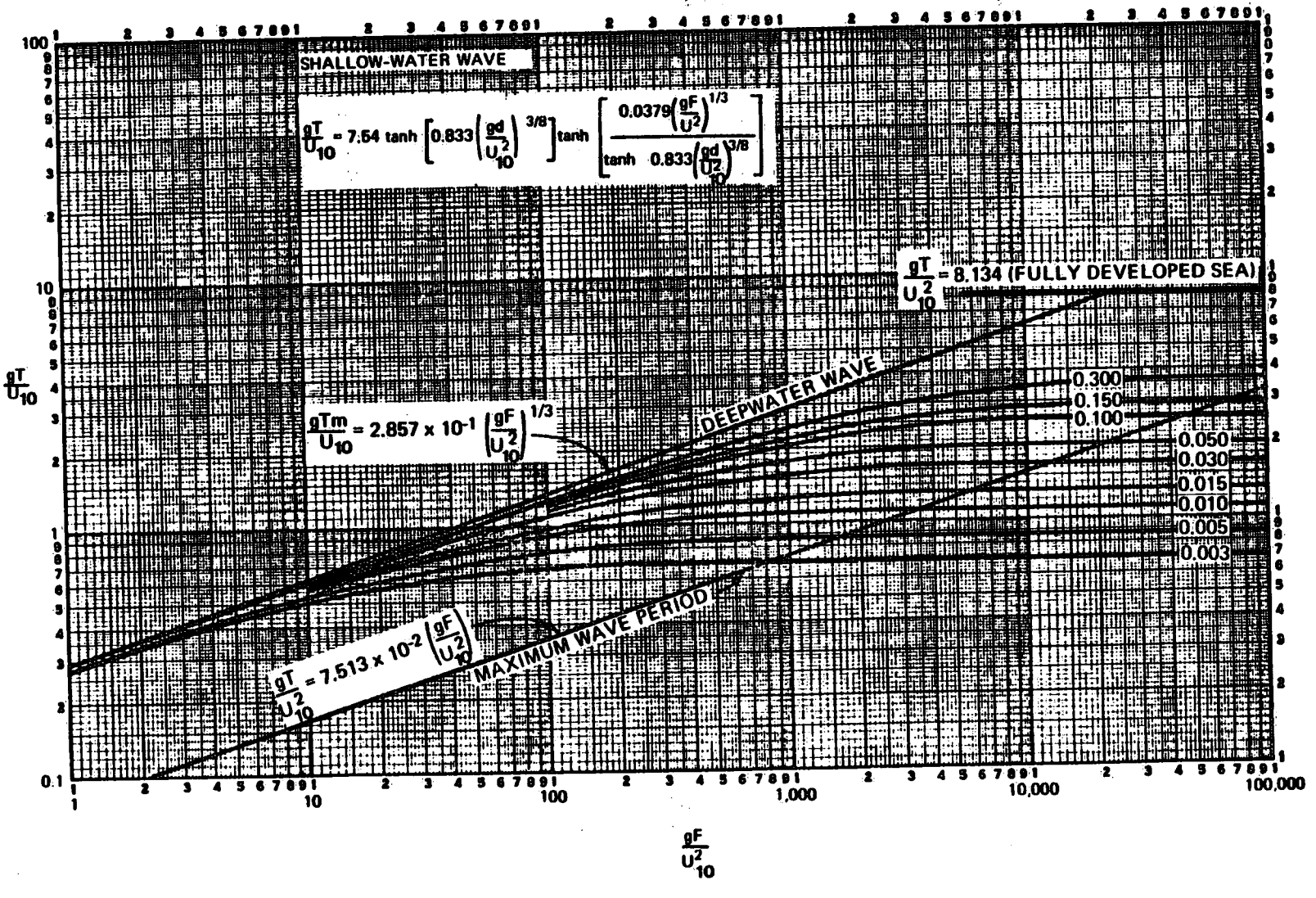

Figure 35. Wave period prediction curves for different values of constant water depth (after Shore Protection Manual 1984).

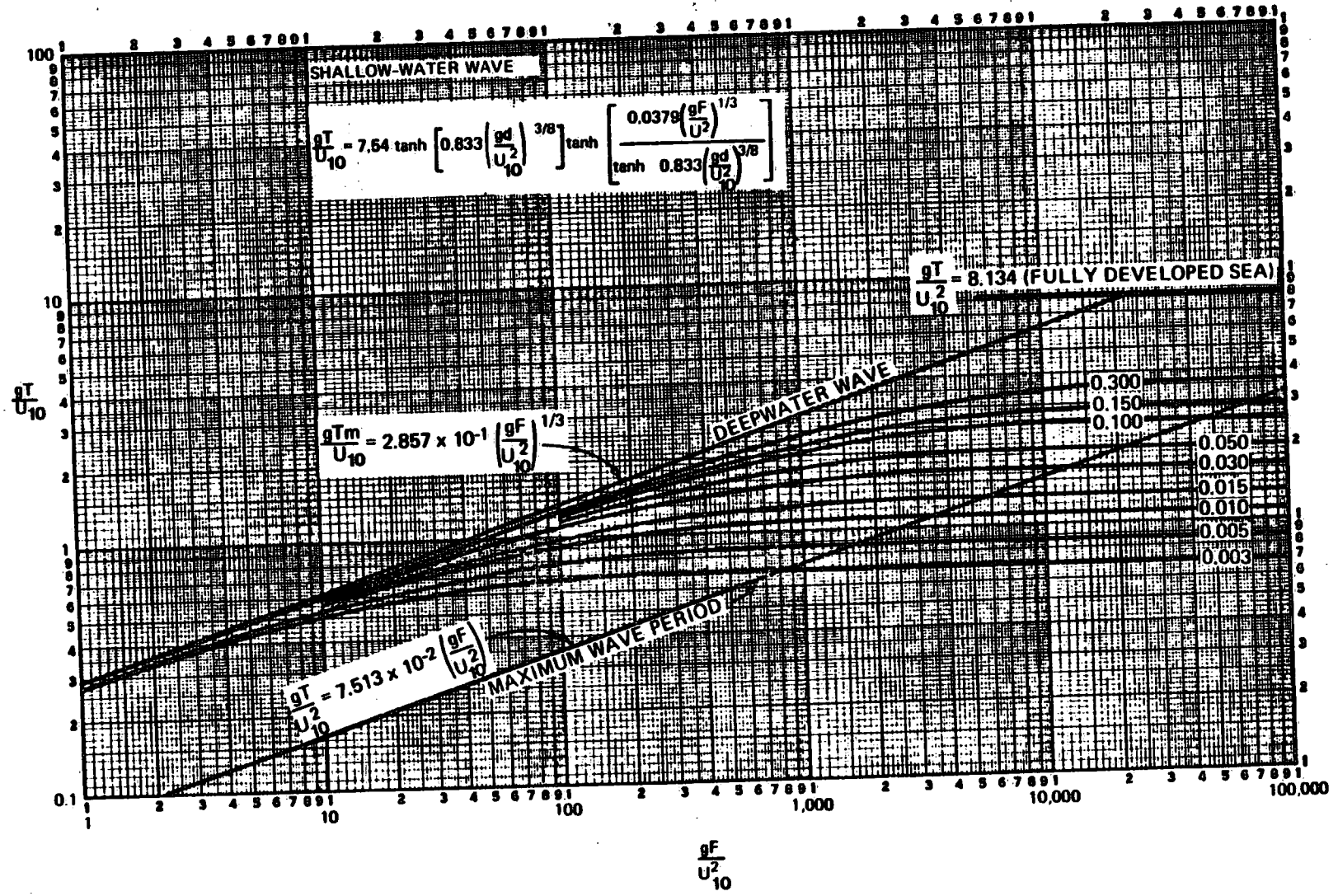

Figure 35. Wave period prediction curves for different values of constant water depth (after Shore Protection Manual 1984).